

9311 0006 NI ACAN

TECH LIBRARY KAFB, NM  
0066123

# NATIONAL ADVISORY COMMITTEE FOR AERONAUTICS

TECHNICAL NOTE 3000

STUDIES OF THE USE OF FREON-12 AS A  
WIND-TUNNEL TESTING MEDIUM

By Albert E. von Doenhoff, Albert L. Braslow,  
and Milton A. Schwartzberg

Langley Aeronautical Laboratory  
Langley Field, Va.



Washington  
August 1953

AFMDC  
TECHNICAL LIBRARY  
AFL 2811



## TECHNICAL NOTE 3000

STUDIES OF THE USE OF FREON-12 AS A  
WIND-TUNNEL TESTING MEDIUMBy Albert E. von Doenhoff, Albert L. Braslow,  
and Milton A. Schwartzberg

## SUMMARY

A number of studies relating to the use of Freon-12 as a substitute medium for air in aerodynamic testing have been made. The use of Freon-12 instead of air makes possible large savings in wind-tunnel drive power. Because of the fact that the ratio of specific heats is approximately 1.13 for Freon-12 as compared with 1.4 for air, some differences exist between data obtained in Freon-12 and in air. Methods for predicting aerodynamic characteristics of bodies in air from data obtained in Freon-12, however, have been developed from the concept of similarity of the streamline pattern. These methods, derived from consideration of two-dimensional flows, provide substantial agreement in all cases for which comparative data are available. These data consist of measurements throughout a range of Mach number from approximately 0.4 to 1.2 of pressure distributions and hinge moments on swept and unswept wings having aspect ratios ranging from 4.0 to 9.0, including cases where a substantial part of the wing was stalled.

The Freon charging and recovery system used for the Langley low-turbulence pressure tunnel is described.

## INTRODUCTION

The relatively large amounts of power required to operate wind tunnels at Mach numbers of the order of 1.0 makes it desirable to investigate the possibility of using some substance other than air as a testing medium. Since the power required to operate a wind tunnel at a given Mach number varies directly as the cube of the velocity, a gas which has a low speed of sound offers the possibility of important savings in power. Freon-12 ( $\text{CCl}_2\text{F}_2$ ) has been used as a testing medium in a number of NACA facilities. The speed of sound in Freon-12 is approximately half that in air; the density at the same temperature and pressure is approximately four times as great, but the absolute

viscosity is approximately the same. Consequently, for a given size model and stagnation temperature and pressure, the Reynolds number corresponding to a given Mach number is approximately twice as large in Freon as it is in air and the power required is half as great. For the case of the Langley low-turbulence pressure tunnel, replacing the air in the tunnel with Freon-12 increased the maximum attainable test-section Mach number from approximately 0.4 to 1.2 without necessitating any increase in the tunnel power or change to the propeller. The maximum pressure at which a Mach number of 1.0 can be attained is 28 inches of mercury absolute, and the corresponding Reynolds number per foot of model chord is  $9.5 \times 10^6$ .

In addition to its primary advantage from the point of view of obtaining high-speed data at high Reynolds numbers with a relatively small amount of power, Freon-12 has a number of other advantages for certain types of investigations. For example, the stresses in a piece of rotating machinery are directly related to the peripheral speed. Consequently, for tests in which a given tip Mach number is required, the stresses and hence the difficulties of fabrication are greatly reduced. The use of Freon also has certain advantages for flutter investigations and investigations of oscillating forces. The lower tunnel speed for a given Mach number reduces directly all pertinent frequencies and consequently simplifies the instrumentation problem involved in measurements of such quantities as aerodynamic damping. Dynamic studies involving gravitational forces (for example, the study of bomb dropping) can be considerably simplified by the use of Freon. The primary conditions for dynamic similarity in this case are identity of the relative density of the dropped object, the Mach number, and the Froude number. The relative density is usually fairly easily adjusted. Since the speed of sound in Freon is approximately half that in air, identity of the Froude number at the same Mach number means that the scale of the model shall be approximately one-quarter that of the prototype. Such similarity with a reduced model scale cannot be obtained with model tests in air.

Any substitute medium to be used for aerodynamic testing must meet a number of practical requirements such as commercial availability at practical cost, chemical inertness, nontoxicity, low vibrational-heat-capacity lag, and low boiling point. The current cost of Freon-12 to the United States Government is approximately 33 cents per pound in two-thousand pound lots. As judged from several years' use in the Langley low-turbulence pressure tunnel, Freon-12 is essentially chemically inert in that no corrosive effects due to the presence of Freon-12 in the tunnel have been detected. The toxicity of Freon-12 is considerably less than that of carbon dioxide. Detailed discussion of toxicity investigations is given in references 1 and 2. In order to avoid additional energy losses not present in air at flow Mach numbers

of the order of 1.0, it is necessary that the vibrational-heat-capacity lag be low. Tests reported in reference 3 indicate that extraneous effects from this source are not to be expected. The boiling point of Freon-12 at atmospheric pressure is about  $-22^{\circ}\text{F}$ . Consequently, at ordinary ambient temperatures, there is little danger of condensation and, as indicated in reference 3, the characteristics of Freon-12 depart only slightly from those of a perfect gas at pressures of 1 atmosphere or less and ordinary ambient temperatures.

The principal difficulty associated with the use of Freon-12 is the fact that the specific-heat ratio  $\gamma$  is only about 1.13 as compared with 1.4 for air so that significant quantitative differences exist between the compressibility relations for air and Freon. For this reason considerable uncertainty has existed concerning the relation between data obtained for a model tested in Freon and data for the same model tested in air.

The studies reported in the present paper were undertaken in an effort to help resolve this uncertainty. Pressure measurements were made for two small nozzles with both air and Freon. In addition, pressure measurements with Freon in the wind tunnel were made for an unswept wing and a wing having  $45^{\circ}$  of sweepback for which corresponding data in air had previously been obtained. Hinge-moment measurements were also made in Freon for an elevator on an unswept tail surface for which corresponding data in air were available.

As will be shown, differences were found to exist between the air and Freon data which became appreciable at transonic stream Mach numbers; however, a simple tentative method based on considerations of flow geometry was developed whereby both Mach number and aerodynamic coefficients are subjected to slight corrections. These corrections brought the Freon and air data into substantial agreement. This method and the various tentative correction curves and procedures based on it are also described and discussed in the present paper. Subsequent data obtained in the Langley low-turbulence pressure tunnel with Freon-12 will, at least for the present, be corrected to corresponding air data by these methods although some modification may be found desirable as additional comparison data in air and Freon accumulate.

In addition to the necessity for applying corrections to aerodynamic data obtained in Freon, the use of this medium has the disadvantage that auxiliary equipment must be supplied to remove the gas from the tunnel or at least a portion of the tunnel before personnel can enter to make model changes or other adjustments. A description of the methods used to introduce and remove Freon from the Langley low-turbulence pressure tunnel as well as necessary changes to the tunnel itself is included in the present paper.

## SYMBOLS

A	stream-tube area or aspect ratio
$\Lambda$	sweep angle of 0.25-chord line of two wing models and of 0.70-chord line of tail-surface model
$\lambda$	taper ratio, ratio of tip chord to root chord
b	span of wing
c	section chord of wing, measured parallel to plane of symmetry of model
H	total pressure
M	Mach number
p	static pressure
P	pressure coefficient, $\frac{p - p_0}{q_0}$
$P_R$	resultant pressure coefficient, $P_L - P_U$
q	dynamic pressure, $\frac{1}{2}\rho V^2$
S	pressure coefficient, $\frac{H_0 - p}{q_0}$
$S_R$	local load coefficient, $S_U - S_L$
V	velocity
x	distance from leading edge along section chord of wing
y	distance normal to free stream in lift direction
$\alpha$	angle of attack
$\gamma$	ratio of specific heat at constant pressure to specific heat at constant volume
$\delta$	correction factor in expression for $C_{D1}$ ; also flap deflection, deg
$\rho$	mass density

$c_d$	wing-section wake drag coefficient
$C_{D_i}$	wing induced-drag coefficient
$C_{D_L}$	wing drag coefficient due to lift
$C_D$	total wing drag coefficient, wake drag coefficient plus induced-drag coefficient or zero-lift drag coefficient plus wing drag coefficient due to lift
$c_h$	section hinge-moment coefficient for flap
$C_h$	elevator hinge-moment coefficient
$C_L$	wing lift coefficient
$C_N$	wing normal-force coefficient
$c_m$	section pitching-moment coefficient about $0.25c$
$c_n$	section normal-force coefficient
$\Delta c_d$	} coefficient in Freon-12 minus corresponding coefficient in air
$\Delta C_{D_i}$	
$\Delta c_h$	
$\Delta C_L$	
$\Delta C_N$	
$\Delta c_m$	
$\Delta c_n$	
$\Delta S_R$	
$\Delta P_R$	

Subscripts:

A        air

F	Freon-12
U	upper surface
L	lower surface
o	conditions in free stream
1	conditions in wake
2	conditions at orifice 2 for nozzle tests
cr	conditions at a local Mach number of 1.0
l	local conditions

## COMPARISON OF NOZZLE FLOWS

### Nozzle Tests

In order to obtain comparative data for some simple two-dimensional flows, pressure-distribution measurements of the flow about two bumps in a 1-inch nozzle were made in both Freon-12 and air. Sketches of the nozzle arrangement and bumps are presented in figures 1 and 2. One of the bumps was rather long and thick. In this case the opposite wall of the nozzle was curved to provide a reasonable margin between the lowest Mach number at which the speed of sound occurred locally and the nozzle-choking condition. The second configuration consisted of a small bump with the opposite wall of the nozzle straight. In each case the gas was forced through the nozzle from large-capacity high-pressure storage tanks. For the Freon tests, in order to avoid conditions close to condensation, the gas was heated before passing through the nozzle into a large evacuated chamber.

The nozzles were cast from bismuth-tin alloy and the surfaces were polished. Pressure tubes were cast into the nozzle and were located as shown in figures 1 and 2. Rubber gaskets, cut to fit the nozzle contours, served to seal the nozzle blocks to glass side walls of the section. Manometer readings were recorded by means of cameras.

The two bumps in the 1-inch-wide nozzle were tested in Freon-12 through a range of Mach number from just below the critical speed to the nozzle-choking speed and then retested in air through a similar range of Mach number. The Reynolds numbers for the air tests were maintained approximately the same as for the Freon tests by adjusting the stagnation pressures to the required values. The values of the absolute stagnation pressure during the Freon and air tests were

approximately 29 and 76 inches of mercury, respectively. The nozzles were not altered in any way between the Freon and air tests.

The Mach number at static orifice 2 (fig. 2) is used as the reference Mach number. If the bump in the nozzle is considered to be crudely representative of an airfoil mounted in a two-dimensional tunnel, the values of local Mach number  $M_2$  at orifice 2 are not free-stream values because of the close proximity of orifice 2 to the bump (fig. 2) but correspond to free-stream Mach numbers that are somewhat higher.

#### Comparison of Results; Streamline-Similarity Concept

The pressure coefficient  $S$  obtained in air and in Freon-12 at each orifice location is plotted against  $M_2$  in figures 3 and 4. These data do not indicate any large differences in results obtained in Freon-12 as compared to those obtained in air except near the maximum Mach number attainable. There is some indication that the Mach number at which choking occurs in Freon-12 is slightly greater than in air.

The differences between the Freon and air results shown in figures 3 and 4 led to more detailed consideration of the relationship between flows in Freon and in air and to the present proposal that a correspondence between the flows might be based more accurately on the concept of geometrical similarity of the streamline pattern than on identity of the Mach number fields. If such streamline similarity exists, the ratio of the stream-tube areas at any two positions for Freon flow must be equal to the ratio of the stream-tube areas at the same positions for air flow. Furthermore, in either gas, the stream-tube area is a minimum when the speed of flow is equal to the local speed of sound. The range of physically possible streamline spacings in either gas may then be represented by values of the ratio  $A_{cr}/A$  ranging from 1.0 to 0.

The variable  $A_{cr}/A$  may be considered a flow parameter in the same sense as the Mach number. The relationship between  $A_{cr}/A$  and the Mach number for air and Freon is given in figure 5 as determined from the relation

$$\frac{A_{cr}}{A} = M \left[ \frac{1 + \frac{\gamma - 1}{2} M^2}{\frac{\gamma + 1}{2}} \right]^{-\frac{\gamma + 1}{2(\gamma - 1)}} \quad (1)$$

It is seen from figure 5 that the variation of  $A_{cr}/A$  with Mach number is very nearly the same for air and Freon-12 up to a Mach number of about 1.4. The differences in  $A_{cr}/A$  increase progressively with increasing Mach number above a value of 1.0.

In order that the same range of streamline spacings be available in both gases, as is necessary if streamline similarity is to be generally possible, it is necessary that the relative streamline spacing be expressed in terms of the variable  $A_{cr}/A$ , where  $A_{cr}$  is the streamline spacing corresponding to a local Mach number of 1.0. If the area at some Mach number other than unity were chosen as the reference area - for example, the area at a Mach number of 0.8,  $A_{0.8}$  - then there would be a range of Mach numbers near unity for which values of  $A_{0.8}/A$  for Freon would exceed the highest possible value of  $A_{0.8}/A$  for air.

#### Streamline Similarity and the Transonic Similarity Rule

An indication of the possibility of the existence of streamline similarity is afforded by a study of the rule for transonic similarity given in reference 4. According to the transonic similarity law, developed for flows in which the local Mach numbers throughout the field are nearly equal to 1.0, if the following substitution of variables is made

$$\xi = \frac{x}{a}$$

$$\eta = \frac{y}{a} [(\gamma + 1)t]^{1/3}$$

$$f(\xi, \eta) = \frac{\phi}{ac^*}$$

where

$x, y$	rectangular coordinates in the physical plane
$a$	half chord of body
$t$	ratio of maximum thickness of body to chord
$\phi$	velocity potential in physical plane
$c^*$	velocity of sound at a local Mach number of 1.0
$\xi$	nondimensional coordinate in stream direction
$\eta$	nondimensional coordinate perpendicular to stream direction
$f(\xi, \eta)$	nondimensional velocity potential

the differential equation of motion becomes

$$\frac{\partial^2 f}{\partial \eta^2} = 2K \frac{\partial f}{\partial \xi} \frac{\partial^2 f}{\partial \xi^2}$$

where

$$K = (1 - M_0) [(\gamma + 1)t]^{-2/3}$$

and

$M_0$  free-stream Mach number

If similar flows are to be obtained in the sense of reference 4,  $K$  must remain constant as  $M_0$ ,  $\gamma$ , and  $t$  are varied. In order to show that a corresponding relation must hold throughout the field of flow, let

$$K_1 = (1 - M_1) [(\gamma + 1)t]^{-2/3}$$

be a quantity analogous to the transonic-similarity parameter  $K$  but formed with the local Mach number  $M_1$  rather than the free-stream Mach number  $M_0$ . It is shown in reference 5 that

$$K_1 = -K^{-2/3} \frac{\partial f}{\partial \xi}$$

Since, for similar solutions,  $\partial f / \partial \xi$  at a given point  $(\xi, \eta)$  in the field of flow is independent of variations of  $M_0$ ,  $\gamma$ , and  $t$ , the value of  $K_1$  formed for any point  $(\xi, \eta)$  in the field must also remain constant.

Since  $K_1$  is a function of three variables,  $M_1$ ,  $\gamma$ , and  $t$  at any point  $(\xi, \eta)$  in the field, it is permissible to assume an arbitrary definite relationship between two of the variables and to adjust the third so that similarity is maintained. With this idea in mind, let

$t = \frac{C_1}{(\gamma + 1)^{1/4}}$  where  $C_1$  is an arbitrary constant. Then,  
 $(1 - M_1) [C_1(\gamma + 1)^{3/4}]^{-2/3}$  or  $(1 - M_1) [C_1^{-2/3}(\gamma + 1)^{-1/2}]$  must be a constant; that is,  $(1 - M_1)$  must vary directly as  $(\gamma + 1)^{1/2}$ .

Consider the relationship between  $M_1$  and  $\gamma$  required for streamline similarity. The equation relating the area ratio, Mach number, and  $\gamma$  is as follows:

$$\frac{A}{A_{cr}} = \frac{\left[1 + \frac{\gamma - 1}{2}(1 - M^*)^2\right]^{\frac{\gamma+1}{2(\gamma-1)}}}{1 - M^*} \left(\frac{2}{\gamma + 1}\right)^{\frac{\gamma+1}{2(\gamma-1)}}$$

where  $M^*$  is  $1 - M_2$ . If this expression is expanded in powers of  $M^*$  and terms containing powers of  $M^*$  greater than 2 are neglected, then

$$\frac{A}{A_{cr}} = \frac{2}{\gamma + 1} M^{*2} + 1$$

As indicated previously, if streamline similarity is to be obtained, the value of  $A/A_{cr}$  at corresponding points in the field must remain unchanged as  $\gamma$  is varied. In accordance with this condition,

$M^{*2} = C_2(\gamma + 1)$ , where the value of  $C_2$  depends on the value of  $A/A_{cr}$  at the particular point in question or  $1 - M_2$  varies directly as  $(\gamma + 1)^{1/2}$ . It is thus seen that streamline similarity is consistent with a special case of the general transonic similarity rule. Strictly speaking, then, streamline similarity to the accuracy of the transonic similarity rule would be obtained in two-dimensional flows in air and

Freon-12 if the body tested in Freon were  $\left(\frac{1 + 1.4}{1 + 1.128}\right)^{1/4}$  or 1.030

times as thick as the body tested in air and the free-stream Mach

number in Freon were  $1 - \left(\frac{1 + 1.128}{1 + 1.4}\right)^{1/2}(1 - M_{0A})$  or  $0.943M_{0A} + 0.057$ .

Because of the small magnitude of the correction to the thickness ratio, it is thought that no appreciable error will result if the model tested in Freon has the same thickness ratio as that for which data are desired in air.

A further indication of the existence of streamline similarity is afforded by a study of the comparative pressure-distribution data presented in figures 3 and 4. At any particular stream speed as indicated by the value of  $M_2$  in Freon, the distribution of values of  $A_{cr}/A$  in Freon can be computed from the basic pressure-distribution data by application of the relations for isentropic gas flow. If streamline similarity is assumed, the values of  $A_{cr}/A$  for air flow will be the same at corresponding points. Reversing the preceding process but using the value of  $\gamma$  appropriate to air permits the corresponding values of local pressure coefficient to be computed for air. If these computed values of the pressure coefficients for air agree with those measured in air, the agreement will be an indication that streamline

similarity exists. The aforementioned procedure has been carried out in the preparation of figures 6 and 7; that is, the Freon data have been converted to equivalent air data. It is to be noted that, in the process of converting from Freon to air through the area-ratio concept, slight changes in local Mach numbers as indicated in figure 5 are necessary. Hence, for example, a local Mach number of 0.80 in Freon is equivalent to a local Mach number of 0.786 in air. The converted Freon data in figures 6 and 7 are in much closer agreement with the actual air data than the corresponding data of figures 3 and 4. In fact the converted Freon data and the air data agree almost within the limits of experimental accuracy.

Another comparison between the flows in Freon and in air is given in figures 8 and 9 in which the distribution of local Mach number over the surface of the bumps is given for several reference Mach numbers  $M_2$ . In these figures the Freon data have been converted to equivalent air data by means of the assumption of streamline similarity; that is, the assumption that local values of  $A_{cr}/A$  would be the same in the two gases. In figures 8 and 9 agreement of local values of  $M$  as between air and Freon, therefore, means that local values of  $A_{cr}/A$  are in agreement. Corresponding runs in air and in Freon compared on the basis of very nearly the same values of converted  $M_2$ , that is,  $A_{cr}/A$  at station 2, exhibited the same distribution of converted  $M$ , that is,  $A_{cr}/A$ , over the rest of the surface. The fact that, almost within the limits of experimental accuracy, the distribution of  $A_{cr}/A$  ahead of and behind the shock is the same when the value of  $A_{cr}/A$  at orifice 2 is the same indicates that, for corresponding values of  $A_{cr}/A$ , the position of the shock is the same and that there is no measurable difference in the effect of the shock on the flow.

#### COMPARISON OF WIND-TUNNEL PRESSURE-DISTRIBUTION DATA

The study described in the preceding section "Comparison of Nozzle Flows" indicated that the assumption of streamline similarity for corresponding flows in air and Freon-12 was a good working hypothesis. It was realized, however, that similarity of flows over a bump in a nozzle is not necessarily a general indication that such flow similarity in air and Freon-12 would exist over bodies such as airfoils and wings, because of the absence of conditions required to determine the circulation and the virtual absence of flow separation in the presence of shocks. In order to obtain representative data to investigate more completely the correspondence of flows in air and Freon-12, measurements were made in Freon-12 in the Langley low-turbulence pressure tunnel of the distribution of pressure over a high-aspect-ratio unswept wing and a sweptback-wing-fuselage model,

both of which had been originally tested in the Langley 8-foot high-speed tunnel. Data for the unswept wing have been published in reference 6.

The unswept wing model was a full-span wing of aspect ratio 9 and taper ratio 0.4, with NACA 65-210 airfoil sections. Static-pressure orifices were located on the upper and lower surfaces at eight spanwise stations: 11-, 20-, 30-, and 43-percent semispan on the left half of the wing and 56-, 64-, 80-, and 95-percent semispan on the right half of the wing. The model was equipped with a 20-percent-chord plain aileron which was undeflected for these tests. A more complete description of the model is presented in reference 6.

The sweptback-wing-fuselage model was a full-span midwing configuration. The wing had the 0.25-chord line swept back  $45^\circ$ , an aspect ratio of 4, a taper ratio of 0.6, and NACA 65A006 airfoils in the stream direction. The fuselage was made by cutting off the rear part of a body of revolution of fineness ratio 12 to form one with a fineness ratio of 10. Static-pressure orifices were located on both wing surfaces at five spanwise stations: 20-, 60-, and 95-percent semispan on the left half of the wing and 40- and 80-percent semispan on the right half of the wing.

Each model was tested in the low-turbulence pressure tunnel as a semispan model mounted off one tunnel wall; whereas each had previously been tested in a full-span arrangement in the Langley 8-foot high-speed tunnel. In the 8-foot high-speed tunnel the unswept wing was mounted on a vertical plate in the center of the tunnel and the swept-wing model was mounted on a sting-supported fuselage. The semispan swept-wing model as tested in the low-turbulence pressure tunnel included a half fuselage. The area of the 8-foot-tunnel test section is about twice that of the low-turbulence pressure tunnel so that the tunnel blocking effects for the tests in the two tunnels were approximately the same.

The models were tested in Freon-12 at approximately the same Reynolds number (about  $2 \times 10^6$ ) and through the same range of Mach number and angle of attack used in the original tests in air. The aileron deflection on the unswept-wing model, which was inadvertently set for the tests of reference 6 at  $-0.3^\circ$  rather than the intended  $0^\circ$ , was maintained at  $-0.3^\circ$  for the tests in Freon-12. The tests consisted of measurements of the pressure distribution at all eight spanwise stations on the unswept wing and the pressure distribution at three of the five spanwise stations on the swept wing (20-, 60-, and 95-percent semispan).

Representative comparisons of the chordwise distribution of pressure over the unswept wing in air and in Freon-12 are presented for subsonic Mach numbers in figure 10. These data were obtained at an angle of attack of  $4^\circ$  at a station 30 percent of the semispan from the root. Although the data of figure 10 are only a small part of the large amount of comparative data obtained for this model, they are representative of the large changes in shape of pressure distribution that occur between subcritical and supercritical Mach numbers and correspond to the highest angle of attack for which published pressure-distribution data are available at Mach numbers greater than 0.9 (ref. 6). The conclusions indicated by an examination of figure 10 are the same as would be obtained from the examination of the remaining mass of comparative data. In this figure the pressure coefficient  $P$  is plotted against chordwise position for Mach numbers of 0.400, 0.850, 0.900, and 0.924. The pressure coefficients and free-stream Mach numbers in Freon have been converted to corresponding air data by means of the assumption of streamline similarity.

A typical example showing the magnitude of the conversion from Freon to air conditions is given in figure 11, which corresponds to the data given for an air Mach number of 0.850 in figure 10. In figure 11, as in the case of the nozzle tests, the converted Freon data are in substantially closer agreement with the corresponding air data than the Freon data reduced in the normal fashion without conversion.

It seems apparent from figure 10 that no significant differences in flow phenomena exist between the air and Freon flow. The rather large changes in the shape of the pressure distribution with relatively small changes in Mach number in air flow are duplicated in the Freon flow. The shocks seem to occur at the same chordwise positions and the pressure distributions for the upper and lower surfaces at a Mach number of 0.9 cross at the same position. The small discrepancies between the Freon and air data noticeable for some of the test conditions can easily be accounted for on the basis of the probable errors in determining free-stream Mach number, measurement of the local pressures, angle of attack, and so forth.

Representative comparisons of the chordwise distribution of pressure over the  $45^\circ$  sweptback wing in air and in Freon-12 are presented in figure 12. The data presented in figure 12(a) are for stations 0.20 and 0.95 semispan from the model plane of symmetry and were obtained at an angle of attack of  $14^\circ$  at Mach numbers of 0.60 and 0.80. The data presented in figure 12(b) are for stations 0.20, 0.60, and 0.95 semispan and were obtained at angles of attack of  $2^\circ$  and  $6^\circ$  at a Mach number of 1.2. The Freon pressure coefficients and free-stream Mach numbers have been converted to corresponding air data by application of the streamline similarity concept to the flow in the free-stream direction. On the sweptback wing, as on the unswept wing,

no noticeable differences in flow phenomena exist between the air and Freon flow either at subsonic or low supersonic speeds. Application of the streamline similarity concept to the flow in the free-stream direction appears to be adequate for practical purposes, at least for aspect ratios of this order. Obviously, for an infinitely long swept wing, consistency should require that the component normal to the leading edge should be used. A more detailed discussion of this subject is presented in a subsequent section.

The wide variety of flow conditions for which application of the streamline similarity concept led to substantial agreement of air and Freon data is to be noted. The conditions investigated include not only transonic flows at moderate angles of attack but also cases of transonic flows with strong shocks in which a large part of the wing area is stalled. The possibility of providing adequate corrections to Freon data obtained at free-stream Mach numbers substantially in excess of 1.2 is uncertain, because under such conditions (as indicated in figure 5) the difference in stream-tube area ratio for the same Mach number becomes large.

#### CONVERSION FACTORS FOR FORCES AND MOMENTS

The previous analysis indicated that the flow phenomena about a body in air could be predicted from measurements made about the same body in Freon-12. More particularly, the analysis indicated that the pressure distribution over a body in one medium could be predicted from the measured pressure distribution in the other medium. Since, however, wind-tunnel measurements frequently consist of the measurement of the over-all forces and moments acting on a body rather than of detailed pressure distributions, some means of interpreting force and moment measurements in Freon-12 in terms of corresponding air data is required.

In order to determine the principal factors affecting the correlation of force and moment measurements, a large quantity of wind-tunnel pressure-distribution data measured in air was converted to equivalent Freon data by means of the streamline similarity concept and the differences between the air and Freon data were studied. It is necessary that a method of force correlation produce results within the accuracy of experimental data through a large range of Mach number, angle of attack, and body shape in order to be useful for projected test programs. For this reason and because the principal aerodynamic forces for an airplane occur on a wing, pressure-distribution data obtained in the Langley 8-foot high-speed tunnel on the NACA 65-210 and the NACA 65A006 airfoils and in the Langley rectangular high-speed tunnel on the NACA 65,3-019 airfoil were used for this analysis. The tests on the NACA 65-210 airfoil, as reported in reference 6, covered

a range of Mach number from 0.4 through 0.925 and the tests on the NACA 65,3-019 airfoil, as reported in reference 7, covered a range of Mach number from 0.43 through 0.74. The data on the NACA 65A006 airfoil were obtained at transonic Mach numbers through 1.0. Both airfoils investigated at subsonic speeds were tested through a range of angle of attack from 0° to 10°, whereas the angle of attack for the transonic tests ranged to 20°. Additional data on the effect of flap deflection on the pressure distribution were available on the NACA 65,3-019 airfoil.

#### Normal Force, Pitching Moments, and Hinge Moments

The pressure distributions taken from the selected test data were converted from air to corresponding pressure distributions in Freon-12 by use of the assumption that the area ratio  $A_{CR}/A$  at each point in the field of flow is the same in both mediums. The procedure used involves the application of the area-ratio curves of figure 5 and the following relation:

$$P = \frac{2}{\gamma M_o^2} \left[ \left( \frac{1 + \frac{\gamma - 1}{2} M_o^2}{1 + \frac{\gamma - 1}{2} M_l^2} \right)^{\frac{\gamma}{\gamma - 1}} - 1 \right] \quad (2)$$

For example, to convert known pressure coefficients at a given free-stream Mach number in Freon-12 to air pressure coefficients, the local Mach numbers corresponding to the known pressure coefficients in Freon-12 are determined by means of equation (2). The free-stream and local Mach numbers in Freon-12 are then converted to air Mach numbers for the same area ratio as determined by figure 5. Equation (2) is again employed with the converted air Mach numbers and the value of  $\gamma$  for air to calculate the air pressure coefficients. The same procedure can be followed to convert air pressure coefficients to equivalent Freon pressure coefficients. For each test condition, the incremental change in the pressure coefficient between air and Freon-12 was calculated at a series of points along the chord for both the upper and lower surfaces of the airfoils. The upper- and lower-surface increments at the same positions along the chord were then subtracted to obtain the load-coefficient increment.

Representative pressure distributions in air and the corresponding distributions of load-coefficient increments between air and Freon-12 for large variations of free-stream Mach number, angle of attack, and flap deflection are shown in figures 13, 14, and 15. The area and

moment integrals of the load-coefficient-increment distributions were used to obtain values of  $\Delta c_n/c_{nF}$ ,  $\Delta c_m/c_{mF}$ , and  $\Delta c_h/c_{hF}$  which were found to be appreciably more dependent upon the free-stream Mach number than upon the magnitudes of the pressures or the shape of the pressure distribution, which varied quite radically with airfoil shape, angle of attack, flap deflection, Mach number, and position of shock. In the angle-of-attack range where the normal-force coefficient is of the same order of magnitude as the lift coefficient, the relative magnitude of the correction to the lift coefficient can be taken to be the same as the correction to the normal-force coefficient. The results of this study of a diversity of airfoil pressure distributions in air are shown in figure 16 where the force and moment increment percentages are plotted against the free-stream Mach number in Freon-12.

The same procedure that was used on the airfoil pressure distributions was also used on the pressure distribution over the flap of the NACA 65,3-019 airfoil to determine the Freon-to-air correlation for hinge moments. As can be seen in figure 16, the percentage increments of  $c_h$  are a function mainly of free-stream Mach number and correlated closely with the airfoil pitching moments. The calculated points farthest from the faired curves in figure 16 usually occurred for such small values of  $c_n$ ,  $c_m$ , and  $c_h$  that the error involved in using the percentage increment from the faired curve rather than the actual calculated value is negligible.

In view of the fact that the changes in pressure coefficient depend in a rather complicated way on local flow conditions, it, at first sight, seems surprising that the magnitude of the conversion factor for normal force, pitching moment, and hinge moment is nearly the same and also that it depends almost entirely on free-stream conditions and is relatively independent of lift coefficient and the shape of the particular body. An explanation of this effect is found from a detailed consideration of the variation of the correction to the local load coefficient with the magnitude of the local load coefficient. Figure 17 is a plot of the variation in the difference between the local load coefficients in Freon and air against the magnitude of the local load coefficient in Freon, for a Freon free-stream Mach number of 0.80. It must be realized that the local load coefficient itself is the difference between the pressure coefficients on the upper and lower surface at a given position. The load coefficient can be varied in two ways. The upper-surface pressure coefficient may be held constant and the local load coefficient increased by decreasing the lower-surface pressure coefficient. Curves corresponding to this method of varying the local load coefficient are shown by the solid lines in figure 17. Conversely, the local load coefficient can be increased by holding the lower-surface pressure coefficient constant and increasing the value of the upper-surface

pressure coefficient. Curves corresponding to this method of varying the local load coefficient are shown by the short-dashed lines in figure 17.

The fact that both the pitching moment and normal force have substantially the same conversion factor (fig. 16) suggests very strongly that each of the local load coefficients along the chord of the airfoil is changed by substantially the same factor. If this were so, the slope of the curve of change in local load coefficient against load coefficient would be constant at a value equal to the conversion factor given in figure 16. This line is shown as the long-dashed line (fig. 17).

It is seen in figure 17 that for low values of the upper-surface pressure (high value of the corresponding pressure coefficient) the general trend of the curve of change in load coefficient against load coefficient is fairly well approximated by the long-dashed line representing the conversion factor of figure 16. Furthermore, regardless of the value of the pressure coefficient, no correction is indicated when the load coefficient is zero. The combinations of pressure coefficient and load coefficient corresponding to corrections at largest variance with that indicated by the long-dashed line are combinations of a relatively low upper-surface pressure coefficient and a large load coefficient. As a matter of general observation, the likelihood of the occurrence of large values of the load coefficient for small values of the upper-surface pressure coefficient is very small. For example, if the upper-surface pressure coefficient is small the corresponding value of the actual pressure is relatively high. Consequently, in order to have a high load coefficient the lower-surface pressure must be very close to the stagnation pressure. Except for conditions in the immediate vicinity of the leading edge, if the lower-surface pressure is near stagnation the corresponding upper-surface pressure is generally quite low, or, in other words, the upper-surface pressure coefficient is quite high. In spite of the fact, therefore, that substantial departures from the general trend are theoretically possible, for the combinations of local pressure coefficient and load coefficient likely to occur in practice the variation of the difference in local load coefficient with load coefficient is nearly linear.

#### Drag (Subsonic)

In order to derive an overall conversion factor to obtain air data from corresponding Freon drag-force test data, it is desirable to consider the subsonic drag as being made up of two parts: (a) that part of the drag associated with the general field of flow - that is, the rearward tilting of the lift vector at the wing due to the effect

of the trailing vortices (induced drag) - and (b) that part of the drag associated with losses of total pressure in the immediate vicinity of the wing. Wake surveys made in the vicinity of the wing would include all of the drag of type (b) but practically none of type (a).

Induced drag.- The induced drag for a wing in subsonic compressible flow is given by the relation (ref. 8):

$$C_{D_i} = \frac{1}{\pi A} (1 + \delta) C_L^2$$

The correction factor  $\delta$  in this expression is a function of the wing geometry and  $\sqrt{1 - M_o^2} \frac{A}{a_o}$  where  $M_o$  is the free-stream Mach number,  $A$  the aspect ratio of the wing, and  $a_o$  the lift-curve slope of the airfoil sections at zero Mach number. Since the differences in Mach number between corresponding flows in Freon and in air are relatively small, the value of  $\frac{1 + \delta}{\pi A}$  can be taken to be the same in air and

Freon at corresponding conditions. The ratio of the induced drag in air to that in Freon, therefore, may be written as

$$\frac{(C_{D_i})_A}{(C_{D_i})_F} = \frac{(C_L^2)_A}{(C_L^2)_F}$$

To the first order, then, the percentage increment in induced drag in converting from Freon to air is equal to twice the percentage increment in lift coefficient or

$$\frac{\Delta C_{D_i}}{(C_{D_i})_F} = 2 \left[ \frac{\Delta C_L}{(C_L)_F} \right]$$

The quantity  $\Delta C_L / (C_L)_F$  can be obtained, as stated previously, from the normal-force increments given in figure 16.

Wake drag.- The wake drag of a body may be associated with flow conditions at a point sufficiently far downstream so that the static pressure has returned to the free-stream value. The method of converting Freon-to-air wake-drag measurements resulted from the assumption that the streamline similarity indicated by the nozzle pressure distributions extended to the region of the wake. The expression for the drag coefficient in terms of quantities that can be measured in the wake is

$$c_d = \frac{2}{c} \int_{\text{wake}} \left( \frac{H_1}{H_0} \right)^{\frac{\gamma-1}{\gamma}} \left[ \frac{1 - \left( \frac{p_0}{H_1} \right)^{\frac{\gamma-1}{\gamma}}}{1 - \left( \frac{p_0}{H_0} \right)^{\frac{\gamma-1}{\gamma}}} \right]^{1/2} \left\{ 1 - \left[ \frac{1 - \left( \frac{p_0}{H_1} \right)^{\frac{\gamma-1}{\gamma}}}{1 - \left( \frac{p_0}{H_0} \right)^{\frac{\gamma-1}{\gamma}}} \right]^{1/2} \right\} dy_1$$

if the static pressure in the wake is taken as free-stream static pressure (ref. 9). The integrand in this expression is, of course,  $d(c_d/2)/d(y/c)$ .

From the assumption of the same stream-tube area ratio  $A_{cr}/A$  in air and Freon both for free-stream conditions and for local conditions in the wake, values of the elemental wake-drag conversion factor

$$\frac{\left[ \frac{dc_d}{d(y/c)} \right]_F - \left[ \frac{dc_d}{d(y/c)} \right]_A}{\left[ \frac{dc_d}{d(y/c)} \right]_F}$$

were computed as a function of  $\left( \frac{H_0 - H_1}{H_0 - p_0} \right)_A$  for various free-stream

air Mach numbers (fig. 18). It is to be noted that for any given free-stream Mach number, the conversion factors for the various points in the wake having different total-pressure losses will be along a line in figure 18 for that particular value of the free-stream Mach number. Because the value of the conversion factor varies much more with the value of the free-stream Mach number than with the loss of total pressure in the wake, it is reasonable to expect that the conversion factor for drag measured in Freon will be primarily a function of the free-stream Freon Mach number and virtually independent of the magnitude of the wake-drag coefficient. By application of the detailed wake-drag conversion factors given in figure 18 to a large variety of air wake-survey data, this condition was actually found to exist. The overall wake-drag conversion factor is plotted against free-stream Freon Mach number in figure 19 for a representative value of

$$\left( \frac{H_0 - H_1}{H_0 - p_0} \right)_A = 0.12.$$

Although the assumption that the stream-tube area ratios are the same for Freon and air may not be as valid when applied to the wake as when applied to the flow over the airfoil profile, the increment in wake drag was shown to reach a value of only 5.2 percent at a free-stream Mach number of 0.9. Inasmuch as this increment is relatively small, it appears that any inadequacies in the basic assumption would result in insignificant differences in the conversion from Freon to air.

Total wing drag.- The Freon-air conversion to the total wing drag coefficient requires that an estimate be made of the relative magnitudes of the wake drag and induced drag. For the purposes of determining the conversion for the total drag, the induced drag can be calculated theoretically. The remainder of the drag as measured on a balance is assumed to be wake drag. This separation of the drag into two components enables the determination of the magnitude of the overall conversion factor. Any error in the estimate of the relative magnitudes of wake and induced drag would result only in a corresponding error in the magnitude of the conversion factor, which in itself is small.

The percentage increments which have been derived for the wake drag and induced drag individually can be combined to convert a total wing-drag coefficient as measured on a balance with the following equation:

$$C_{D_A} = K C_{D_F} + (K' - K) C_{D_{i_F}}$$

where

$$K = 1 - \frac{\Delta c_d}{c_{d_F}}$$

$$K' = 1 - 2 \frac{\Delta C_L}{C_{L_F}}$$

#### Drag (Supersonic)

The fact that the concept of induced drag at subsonic speeds, which is associated with the rearward tilting of the lift vector due to the trailing vortices, loses its meaning at supersonic speeds raises some question as to the method to be employed in converting Freon-12 drag data to air data at Mach numbers above 1.0.

Because of the uncertainty regarding the meaning of induced drag in the aforementioned sense at supersonic speeds, it is more convenient to resolve the total drag at supersonic speeds in a different manner. The total drag may be considered to be composed of a pressure drag and a skin-friction drag. Because the wings considered for use at supersonic speeds are thin and because the leading-edge suction is generally small at transonic and supersonic speeds, it is reasonable to assume that the resultant pressure force on this type of wing is perpendicular to the chord plane and that, for the purpose of determining the Freon-to-air pressure-drag conversion factor,  $C_{D_L} \approx C_N \alpha$ . With the assumption that the resultant pressure force is perpendicular to the chord plane, all the drag at  $C_N = 0$  can be considered to be skin-friction drag. This skin-friction drag is further assumed to remain constant with changes in angle of attack. This latter component of the total drag would always be completely included in a wake survey at  $C_N = 0$ . The method of conversion of Freon total drags to air drags at supersonic speeds is then to apply the wake-drag conversion factors (fig. 19) to the zero-lift drag, and the normal-force conversion factors (fig. 16) to the remainder of the drag. Any inaccuracies which may exist in the preceding method of analyzing the total drag in a supersonic flow can result in only negligible errors in the conversion of Freon total drags to air total drags, inasmuch as the normal-force conversion factors and the wake-drag conversion factors differ by a maximum of only a few percent over the Mach number range considered.

The preceding assumptions, on which the supersonic drag conversion factors depend, are equally applicable at subsonic speeds for thin wings when the leading-edge suction is small. It is desirable, therefore, to compare the results of both conversion methods at subsonic speeds. A quantity of available Freon total-drag data, obtained at high subsonic speeds, was converted to corresponding data in air by both methods of analysis. The converted total-drag data obtained by both methods differed by a maximum of less than two percent. Inasmuch as the conversion method involving an estimate of the induced drag is more generally applicable at subsonic speeds, it is believed that this method should be generally used under such conditions.

#### Rolling Moment, Yawing Moment, and Side Force

The moment of a wing about a longitudinal axis is a function only of the normal force acting on the wing for a constant center of pressure. The spanwise section normal-force coefficients over the wing for any given free-stream Mach number are all converted by the same percentage increment (fig. 16) so that the center-of-pressure location is the same for both air and Freon-12. The conversion factor for the normal-force coefficient, therefore, can be used to convert

rolling-moment coefficients measured in Freon-12 to corresponding coefficients in air.

The yawing-moment and side-force conversion factors will depend upon the nature of the forces involved and consequently may vary for different configurations. For example, the yawing moment contributed by a deflected rudder is caused by a pressure force acting on the vertical tail surface and the conversion of the yawing-moment coefficient from Freon-12 to air should be made, therefore, by application of the normal-force conversion factor. On the other hand, a yawing moment may be caused by asymmetrical skin-friction forces, in which case the moment should be converted from Freon-12 to air by application of the wake-drag conversion factor. The conversion of yawing moment and side force, therefore, should be determined for each individual configuration after consideration of the source of the forces involved.

#### Application to Swept Wings

The application of the streamline-similarity criterion to the flow over swept wings is not quite as apparent as the application to the flow over unswept wings. It is not obvious whether the area-ratio criterion should be applied to the simple sweep theory, that is, to the flow normal to the wing leading edge, or whether it should be applied to the flow in the stream direction. An inconsistency in results exists between the simple sweep theory and a rigid application of the area-ratio concept. Inasmuch as the actual flow over a swept wing of reasonably low aspect ratio is a combination of the two types of flow, for simplicity in applying the conversion from Freon to air, application of the area-ratio concept to the flow in the free-stream direction will be used. As indicated in a previous section from a comparison of experimental data obtained in Freon and in air on a swept wing, the application of the area-ratio concept to the flow in the free-stream direction appeared to be adequate for practical purposes.

In order to obtain an indication of the magnitude of the differences involved in the application of the streamline-similarity concept to the stream flow rather than the flow normal to the wing leading edge, consider the flow about a wing swept back  $45^\circ$  at a Freon free-stream Mach number of 0.9. Application of the streamline-similarity concept to the stream direction and to the normal flow indicates that the values of free-stream Mach number in air are 0.894 and 0.884, respectively. Although this difference in Mach number increases with sweep angle, the importance of an error in the actual free-stream Mach number decreases with sweep inasmuch as the effect of changes in Mach number on the aerodynamic characteristics in the transonic range is appreciably reduced as the sweep is increased. The conversion factor

for the normal-force coefficient for the  $45^\circ$  swept wing at a Freon free-stream Mach number of 0.9 is 7.3 percent when based on the stream flow and 5.0 percent when based on the normal flow. Inasmuch as the flow over a swept wing of relatively low aspect ratio is a combination of the two types of flow, as mentioned previously, the correct value of the conversion factor for such a wing is probably between the two extremes indicated.

#### Critical Check of Conversion Methods

Inasmuch as any possible differences between flow conditions in Freon and in air might be expected to be of the largest magnitude near the trailing edge of a body, it was considered that a critical check of Freon data could be obtained by a comparison of the hinge moments of a trailing-edge control surface measured in Freon and in air. Furthermore, such a comparison would also serve as a check on the method of converting moments described in the preceding section. The tail-surface model used for this comparison was a full-span unswept tail of aspect ratio 4.01 and taper ratio 0.5 with NACA 65-108 airfoil sections and was equipped with a 0.30-chord sealed, unbalanced elevator. More detailed information on this model is presented in reference 10.

A comparison with air data of the hinge-moment measurements made on the tail-surface model in Freon are presented in figure 20 for a range of Mach numbers from 0.775 to 0.907 for various angles of attack and control-surface deflections. An indication of the degree of accuracy of the data is presented in figure 21 where the hinge-moment data obtained in air in both the Langley 8-foot high-speed tunnel and in the Langley low-turbulence pressure tunnel at a Mach number of 0.400 are compared. It is apparent in figure 20 that the agreement of the Freon and air hinge-moment data is substantially as close as the corresponding comparative measurements made only in air (fig. 21). Thus, in every case in which comparative data in Freon-12 and in air are available excellent agreement has been obtained.

#### MODIFICATIONS TO THE LANGLEY LOW-TURBULENCE PRESSURE TUNNEL FOR THE USE OF FREON-12

Several modifications have been made to the Langley low-turbulence pressure tunnel since a description of it was published in reference 11. It may be of interest here to mention some of these changes and to describe the characteristics of the modified tunnel.

The primary physical change to the tunnel air passage has been the installation of a new test section to permit testing in Freon-12 at high subsonic Mach numbers. The original section had constrictions upstream and downstream of the test region which had to be removed for tests at high Mach numbers. The size of the new test section is essentially the same as the original but the side walls are expanded to allow for the growth of the wall boundary layer. The longitudinal distribution of Mach number along the tunnel center line is presented in figure 22. Each curve, of course, is for a different propeller rotational speed. The data indicate that the side walls are expanded sufficiently to obtain a uniform distribution of Mach number through the test section up to a Mach number of about 0.97. The original drive motor and propeller are being used and with these it is possible to choke the tunnel, as evidenced in figure 22 by the region of supersonic flow at the highest test Mach number.

When Freon-12 is used as a testing medium, the Mach number and Reynolds number can be varied independently simply by changing the stagnation pressure of the Freon. The Mach number can be increased to the tunnel choking condition for a range of absolute stagnation pressure from approximately 6 to 28 inches of mercury and the range of Reynolds number that can be covered at each Mach number is correspondingly large. For example, at a Mach number exceeding 0.9, the Reynolds number range is from approximately  $2.5 \times 10^6$  to  $9.5 \times 10^6$  per foot of chord.

A 60-mesh screen and two of the original eleven turbulence-reducing 30-mesh screens (ref. 11) have been removed. In addition, boundary-layer suction slots in the test-section side walls have been removed. These alterations have increased the energy ratio of the tunnel somewhat but have not caused any noticeable increase in the low turbulence level, as evidenced by measurements of the critical boundary-layer Reynolds number on the same airfoil model in both test sections; at the same chordwise position, the same critical boundary-layer Reynolds number was measured in both test sections.

In order to provide for comparisons with data previously obtained in air at a Mach number of 1.2, a temporary modification to the test section of the Langley low-turbulence pressure tunnel to permit testing in Freon-12 at a Mach number of 1.185, corresponding to a Mach number of 1.2 in air, was developed by the method of characteristics. The modification consisted of a plaster nozzle liner built up on the side walls of the tunnel test-section entrance cone, smoothed and faired with a plastic coating to conform to the design specifications.

The Mach number distribution through the test section, presented as air values converted from the Freon data, is shown in figure 23.

The actual free-stream Mach number, as converted from Freon to air, in the region of the model used for the supersonic tests is seen to correspond more closely to an average value of 1.205 than to the design value of 1.2. For the comparison purposes employed, any such slight difference in the air free-stream Mach number is negligible.

#### FREON CHARGING AND RECOVERY SYSTEM USED FOR THE LANGLEY LOW-TURBULENCE PRESSURE TUNNEL

For obvious reasons, provisions must be made for storage of the Freon removed from the tunnel and for separating this Freon from an air-Freon mixture with a minimum loss. The degree of separation attainable and the capacity of the equipment represent a compromise between convenience of operation and cost. The volume of the Langley low-turbulence pressure tunnel is 83,000 cubic feet. Because most entries into the tunnel during the course of a typical investigation are for the purpose of making minor adjustments or changes to the model, the test chamber is separated from the return passage of the tunnel by means of gas-tight gates. The volume which has to be evacuated, then, for making short entries has been thereby reduced to 12,000 cubic feet.

Equipment having an intake capacity of 1700 cubic feet per minute was chosen. This capacity is sufficient to handle the volume of the test chamber in 12 minutes and to handle the volume of the complete tunnel in 84 minutes. Of course, to remove completely Freon from a given volume requires that the gas in the volume be passed through the equipment more than once because of mixing. Furthermore, the full capacity of the equipment is available only when the absolute pressure in the tunnel is approximately 10 inches of mercury or less. Consequently, the average time required for removing or introducing Freon-12 to the test chamber only is about 30 to 45 minutes, and the corresponding time for this process for the complete tunnel is about 4 hours.

A simplified block diagram showing the essential components of the system is given in figure 24. In order to introduce Freon into the tunnel, the tunnel is first evacuated from the highest point through a 75-horsepower vacuum pump to an absolute pressure of 2 or 3 inches of mercury. Pure Freon gas is then introduced in the bottom of the tunnel from the Freon storage tank at a rate equal to the capacity of the vacuum pump. The latent heat required to vaporize the liquid Freon is supplied by 580-kilowatt heaters. The operation is continued, with the output of the vacuum pump discharging to atmosphere until traces of Freon are found in the vacuum-pump exhaust. The exhaust is then valved to the intake of a four-stage single-unit 300-horsepower piston

compressor and compressed to an ultimate pressure of 1800 pounds per square inch. The discharge of each stage is passed through a water-cooled condenser. The temperature of the gases after the first and second stages of the piston compressor is controlled so that no Freon will condense. Most of the Freon is condensed after the third stage where the pressure is sufficiently high to force the liquid Freon into the storage tank without difficulty. In order to avoid unbalancing of the machine, gaseous remnants from the fourth stage are reintroduced to the output of the third stage, thus compensating for the volume of the Freon condensed. The output of the system is passed through a cooler in which the temperature is maintained at  $-50^{\circ}$  F at a pressure of 1800 pounds per square inch. Since the partial pressure of Freon-12 at this temperature is 7 pounds per square inch, the mixture discharged to atmosphere should contain Freon only to the extent of 7/1800 parts by volume. The low temperature in the final cooler is maintained by a separate refrigeration system in which Freon-12 is used as the refrigerant. The process is stopped when the desired purity of Freon in the wind tunnel is attained. A corresponding procedure is followed in removing Freon from the tunnel.

The purpose of the heater in the liquid line from the  $-50^{\circ}$  F cooler indicated in figure 24 is to prevent freezing of any water condensed in the preceding stages. In the early periods of operation of the system, difficulties were experienced because of the presence of water vapor and condensed water. It is readily understood that substantially all water vapor must be eliminated before the gases enter the  $-50^{\circ}$  F cooler. In addition, however, although no corrosive effects of Freon-12 have been noted in the wind tunnel, excessive rates of corrosion were found to occur in the warmer portions of the 1800-pounds-per-square-inch piping if water were not eliminated. Apparently, the liquid Freon has a tendency to remove the normally present protective oil coating and the high oxygen concentration at 1800 pounds per square inch in the presence of water then rapidly corroded the pipes. To avoid this difficulty, an additional activated alumina drier was placed in the 546-pounds-per-square-inch line.

Although, as mentioned previously, the final cold air-Freon mixture should contain only 0.39 percent Freon-12 by volume, the actual composition of the air-Freon mixture discharged to atmosphere is approximately 2-percent Freon by volume. Apparently, at high pressures, Freon-12, although condensed, has a tendency to remain suspended in the air as a mist and thus more than the theoretical amount is discharged with the air. It is believed that, if the system were redesigned, it would be more effective to decrease the final pressure but also decrease the final temperature. It would probably be possible to realize more nearly the same theoretical recovery with a final pressure of about 600 pounds per square inch and a final temperature of about  $-90^{\circ}$  F which could be obtained with a Freon-22 refrigeration system. No difficulties have

been experienced in obtaining the theoretical recovery with the present system at a pressure of 600 pounds per square inch.

The time required to change from air to Freon or vice versa and the loss of Freon are dependent on the amount of mixing between the two gases during the tunnel charging or purging cycles. The mixing of air and Freon was minimized by taking full advantage of the fact that Freon-12 is much denser than air. The Freon is always introduced or withdrawn at the lowest possible point in the tunnel and air is introduced or withdrawn at the highest possible point. Furthermore, precautions are taken to insure that the velocity of the entering gas is always very low. This is accomplished by means of baffle boxes having areas of approximately 12 square feet, which reduce the velocities to a maximum of less than 3 feet per second. Precautions are taken to insure that no large unvented volumes are left in the tunnel that would trap air or Freon. Occasionally, Freon entering the tunnel has been incompletely vaporized and appeared as a fog. As seen through windows in the tunnel, the mixing zone between air and Freon did not appear to be over 6 inches thick. Of course, all blowers and fans located inside the tunnel are not operated during charging or purging cycles.

The purity of the Freon in the Langley low-turbulence pressure tunnel is found by measuring the velocity of sound which varies linearly with the composition of the mixture by weight. A schematic diagram of the method employed is given in figure 25. Light shining through an aperture in a constant-speed rotating disk onto a photoelectric cell generates a square wave impulse. After going through a differentiating circuit so as to increase the sharpness of the wave front, the impulse is supplied to a speaker located in the tunnel. The impulse from the speaker passes by two microphones a known distance apart. The impulses from the microphones actuate individually two neon lights located at different fixed positions at the perimeter of the rotating disk. The effect is stroboscopic and the time of passage of the wave front from the first to the second microphone is directly related to the difference in reading of graduations on the rotating disk made visible under each light. The speaker and the microphones are located in a sound-proof box which is supplied with samples of the mixture from various parts of the tunnel. With this system, the speed of sound in Freon-12 is measured with an accuracy of about 1/2 percent. As a matter of general operating procedure, the purity of the Freon in the wind tunnel is maintained at or above 90 percent by weight.

## CONCLUDING REMARKS

A number of studies relating to the use of Freon-12 as a substitute medium for air in aerodynamic testing have been made. The use of Freon-12 instead of air makes possible large savings in wind-tunnel drive power. Because of the fact that the ratio of specific heats is approximately 1.13 for Freon-12 as compared with 1.4 for air, some differences exist between data obtained in Freon-12 and in air. Methods for predicting aerodynamic characteristics of bodies in air from data obtained in Freon-12, however, have been developed from the concept of similarity of the streamline pattern. These methods, derived from consideration of two-dimensional flows, provide substantial agreement in all cases for which comparative data are available. These data consist of measurements throughout a range of Mach number from approximately 0.4 to 1.2 of pressure distributions and hinge moments on swept and unswept wings having aspect ratios ranging from 4.0 to 9.0 including cases where a substantial part of the wing was stalled.

Langley Aeronautical Laboratory,  
National Advisory Committee for Aeronautics,  
Langley Field, Va., August 6, 1953

## REFERENCES

1. Sayers, R. R., Yant, W. P., Chornyak, John, and Shoaf, H. W.: Toxicity of Dichloro-Difluoro Methane: A New Refrigerant. R. I. 3013, U. S. Bur. Mines, Dept. Commerce, May 1930.
2. Nuckolls, A. H.: The Comparative Life, Fire, and Explosion Hazards of Common Refrigerants. Misc. Hazard No. 2375, Underwriters' Labs., Inc., Nov. 13, 1933.
3. Huber, Paul W.: Use of Freon-12 As a Fluid for Aerodynamic Testing. NACA TN 1024, 1946.
4. Kaplan, Carl: On Similarity Rules for Transonic Flows. NACA Rep. 894, 1948. (Supersedes NACA TN 1527.)
5. Kaplan, Carl: On a Solution of the Nonlinear Differential Equation for Transonic Flow Past a Wave-Shaped Wall. NACA Rep. 1069, 1952. (Supersedes NACA TN 2383.)
6. Whitcomb, Richard T.: Investigation of the Characteristics of a High-Aspect-Ratio Wing in the Langley 8-Foot High-Speed Tunnel. NACA RM L6H28a, 1946.
7. Lindsey, W. F.: Effect of Compressibility on the Pressures and Forces Acting on a Modified NACA 65,3-019 Airfoil Having a 0.20-Chord Flap. NACA WR L-76, 1946. (Formerly NACA ACR 15G31a.)
8. Goldstein, S., and Young, A. D.: The Linear Perturbation Theory of Compressible Flow, With Applications to Wind-Tunnel Interference. R. & M. No. 1909, British A.R.C., 1943.
9. Heaslet, Max A.: Theoretical Investigation of Methods for Computing Drag From Wake Surveys at High Subsonic Speeds. NACA WR W-1, 1945. (Formerly NACA ARR 5C21.)
10. Bielat, Ralph P.: Investigation at High Speeds of a Horizontal-Tail Model in the Langley 8-Foot High-Speed Tunnel. NACA RM L6L10b, 1947.
11. Von Doenhoff, Albert E., and Abbott, Frank T., Jr.: The Langley Two-Dimensional Low-Turbulence Pressure Tunnel. NACA TN 1283, 1947.

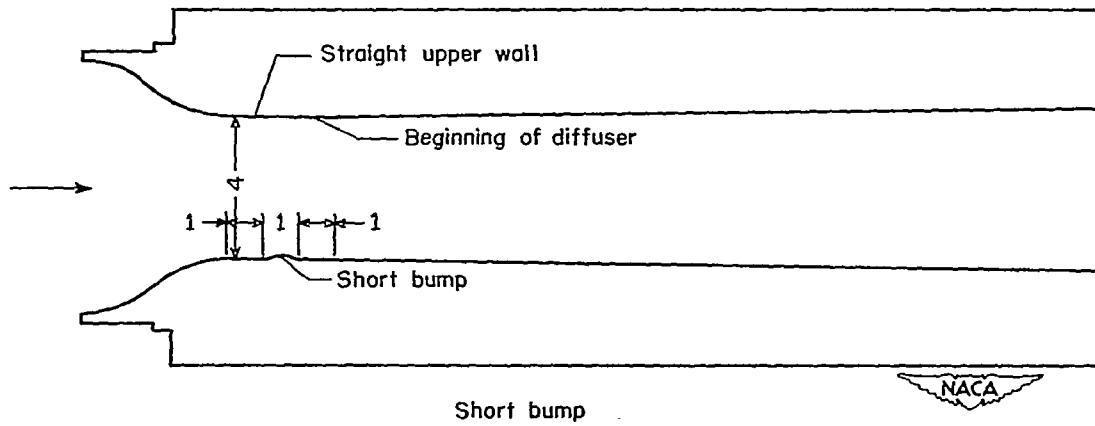
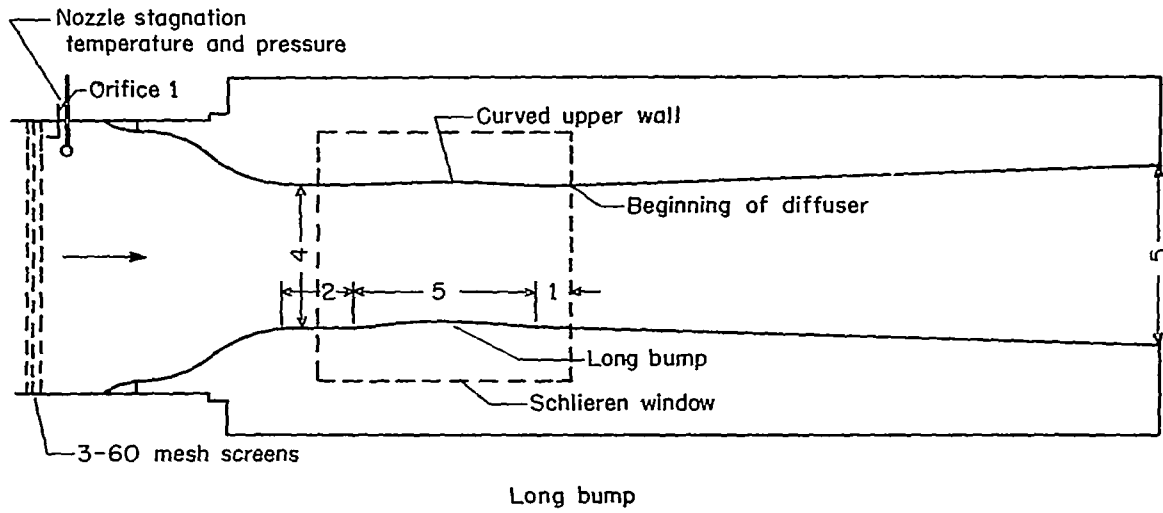


Figure 1.- Elevations of 1-inch-wide nozzle showing location of long and short bumps. (All dimensions in inches.)



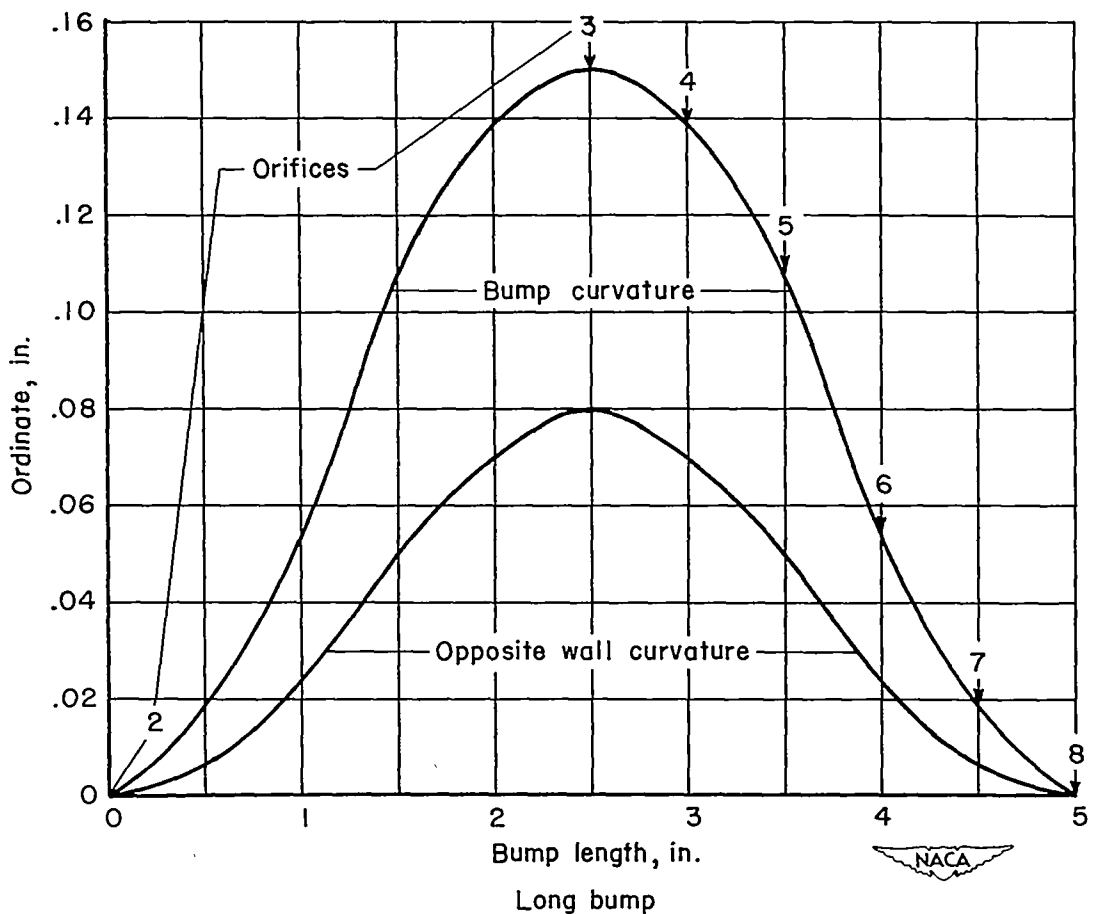
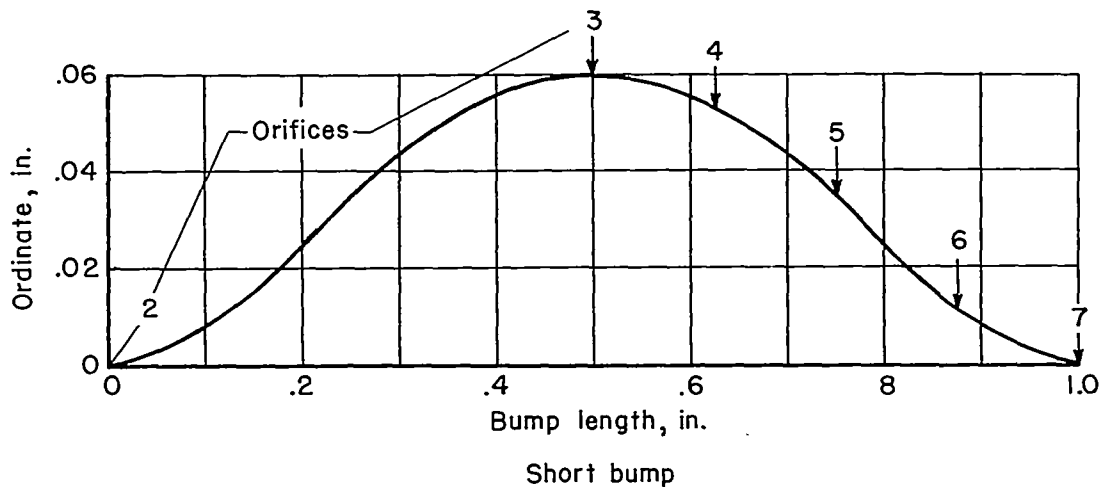


Figure 2.- Sketches of bumps showing location of orifices.

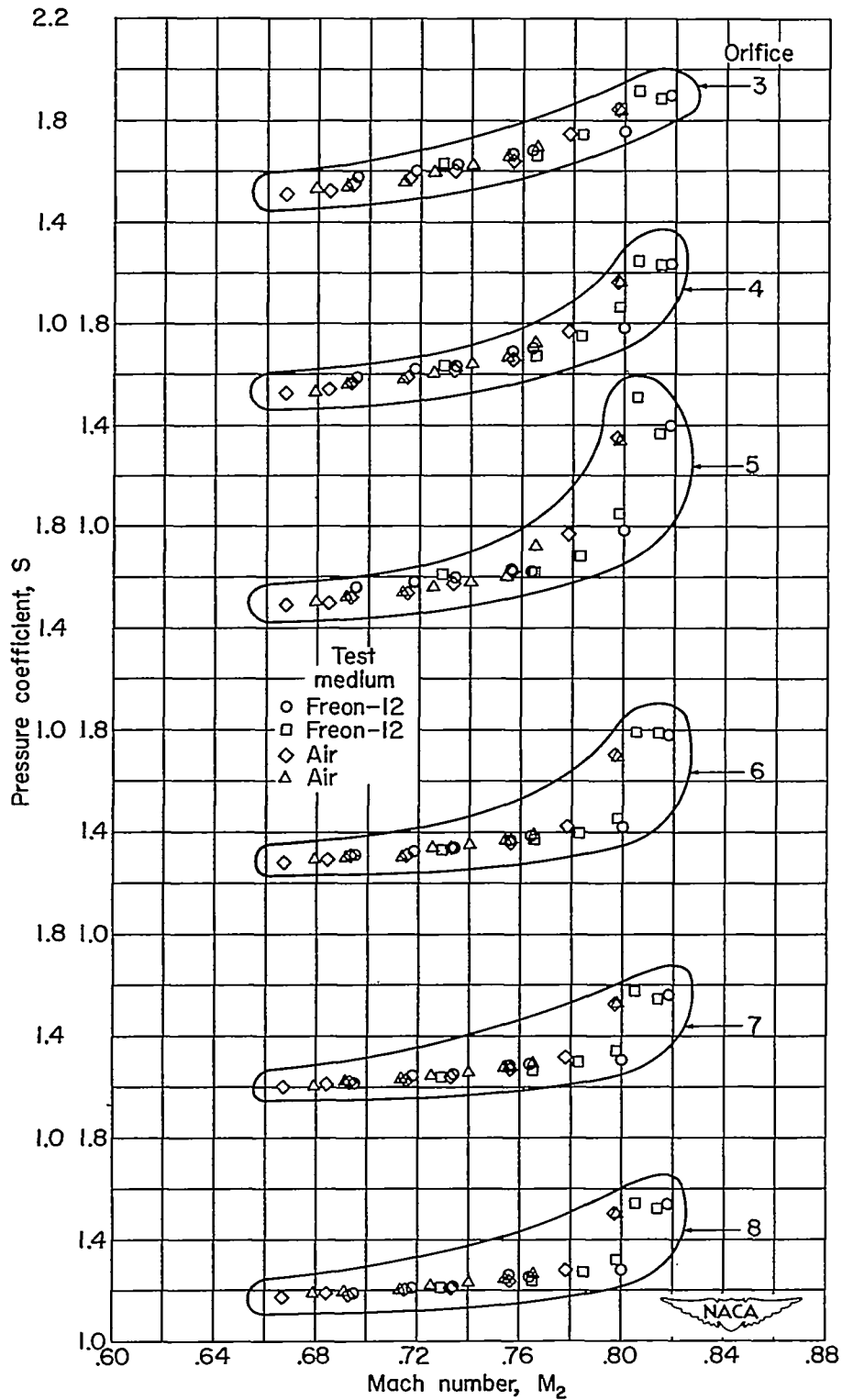


Figure 3.- Variation of pressure coefficient with  $M_2$  at each orifice location along the long bump.

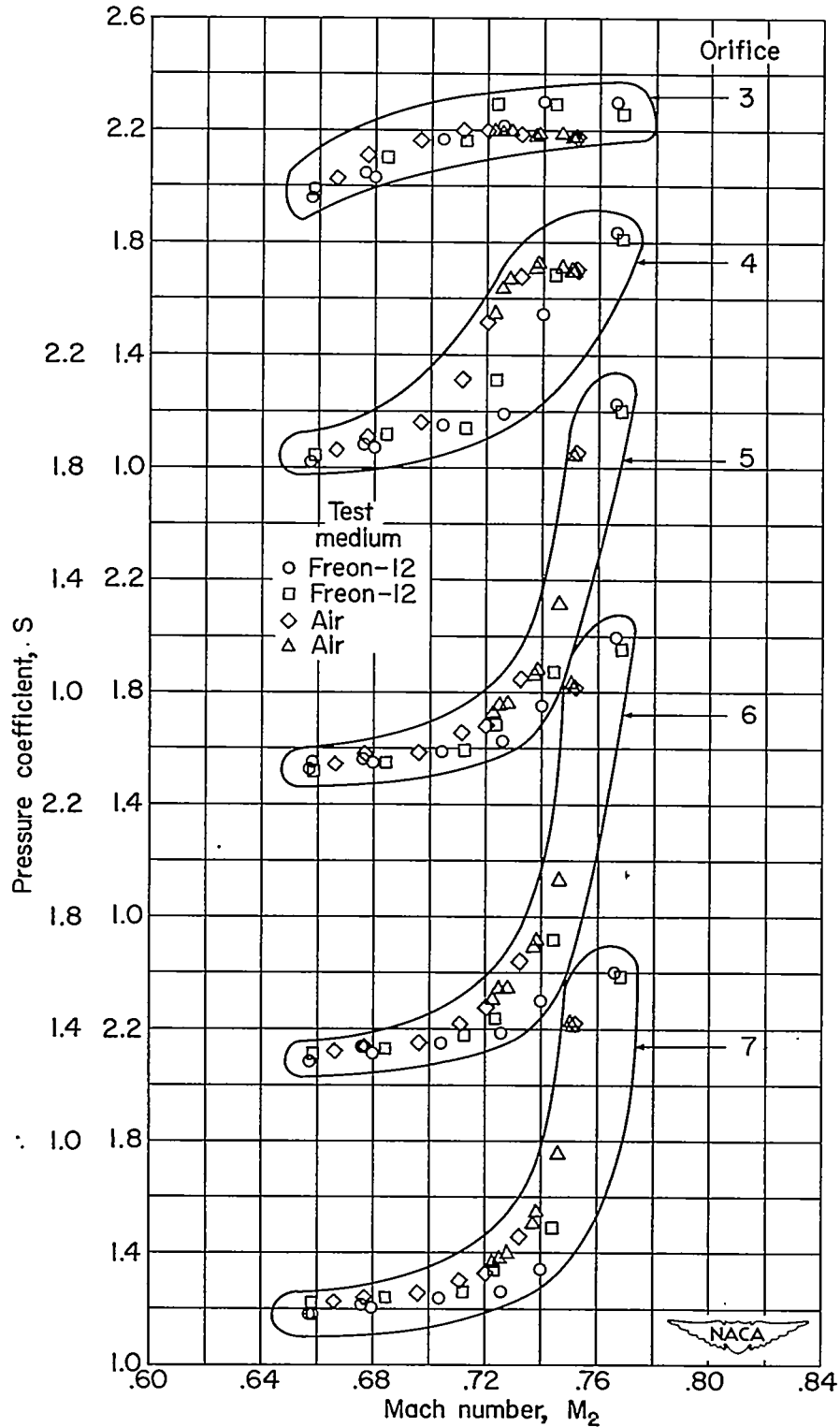


Figure 4.- Variation of pressure coefficient with  $M_2$  at each orifice location along the short bump.

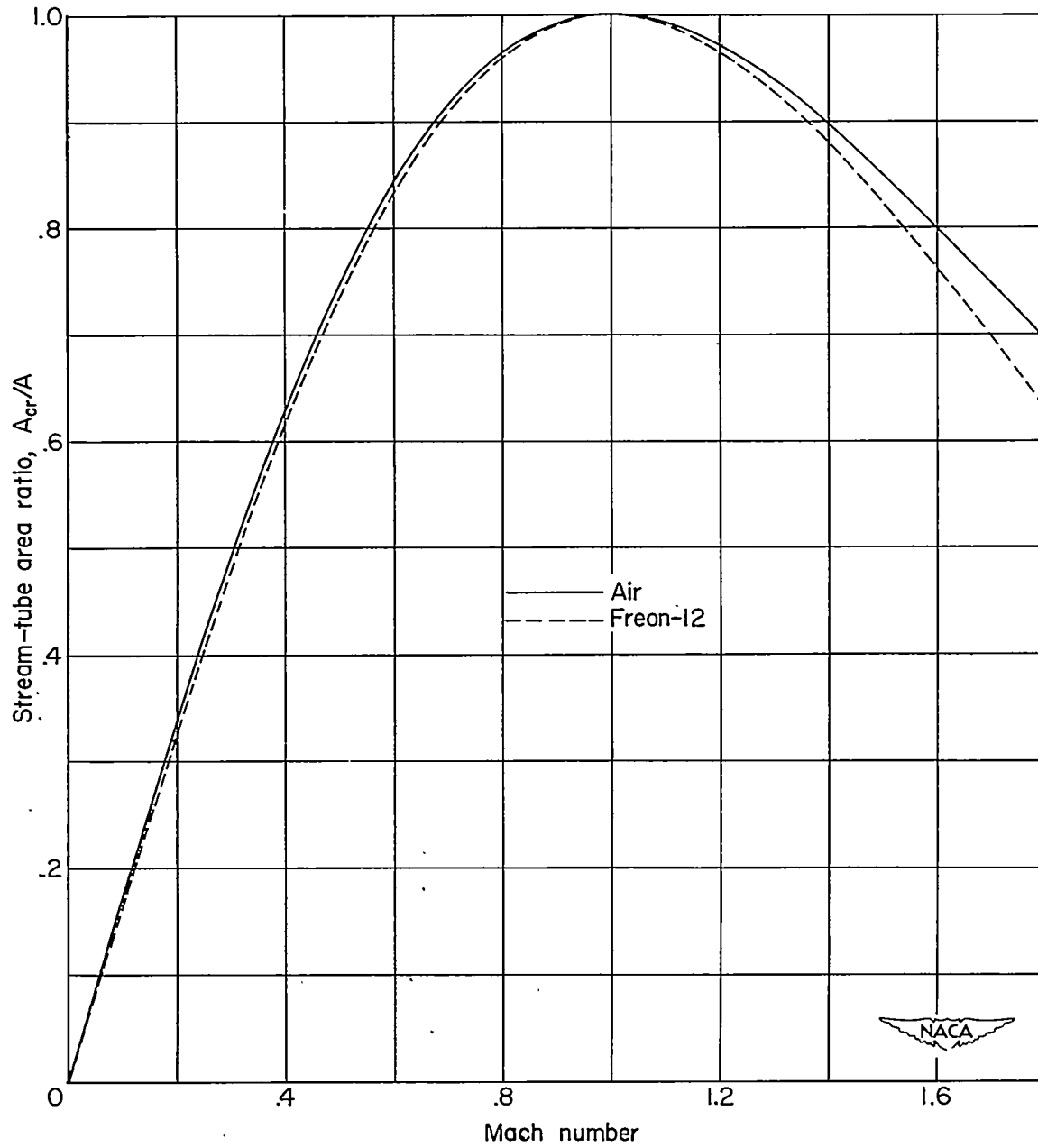


Figure 5.- Variation of stream-tube area ratio with Mach number.

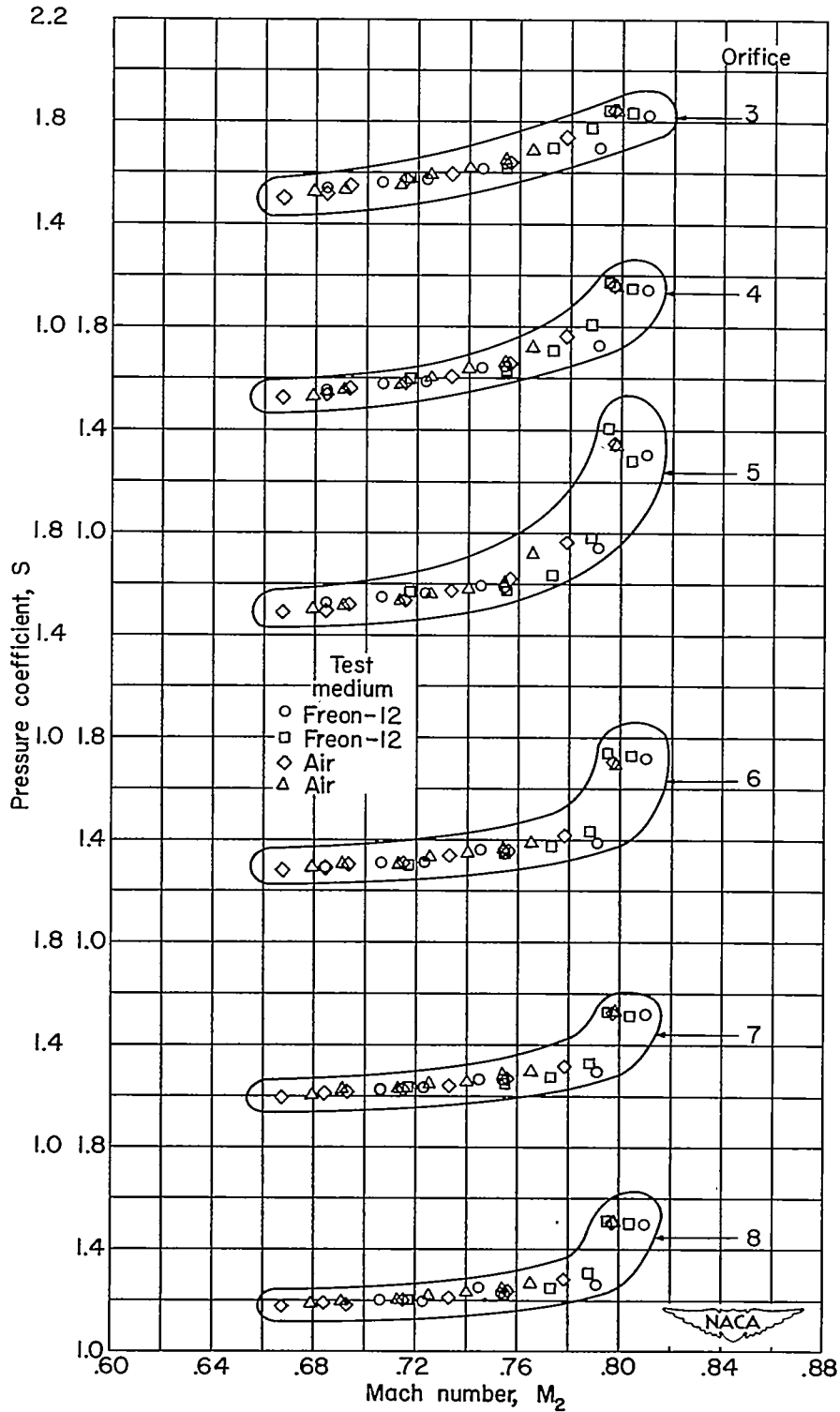


Figure 6.- Variation of pressure coefficient with  $M_2$  at each orifice location along the long bump. Freon data converted to equivalent air values.

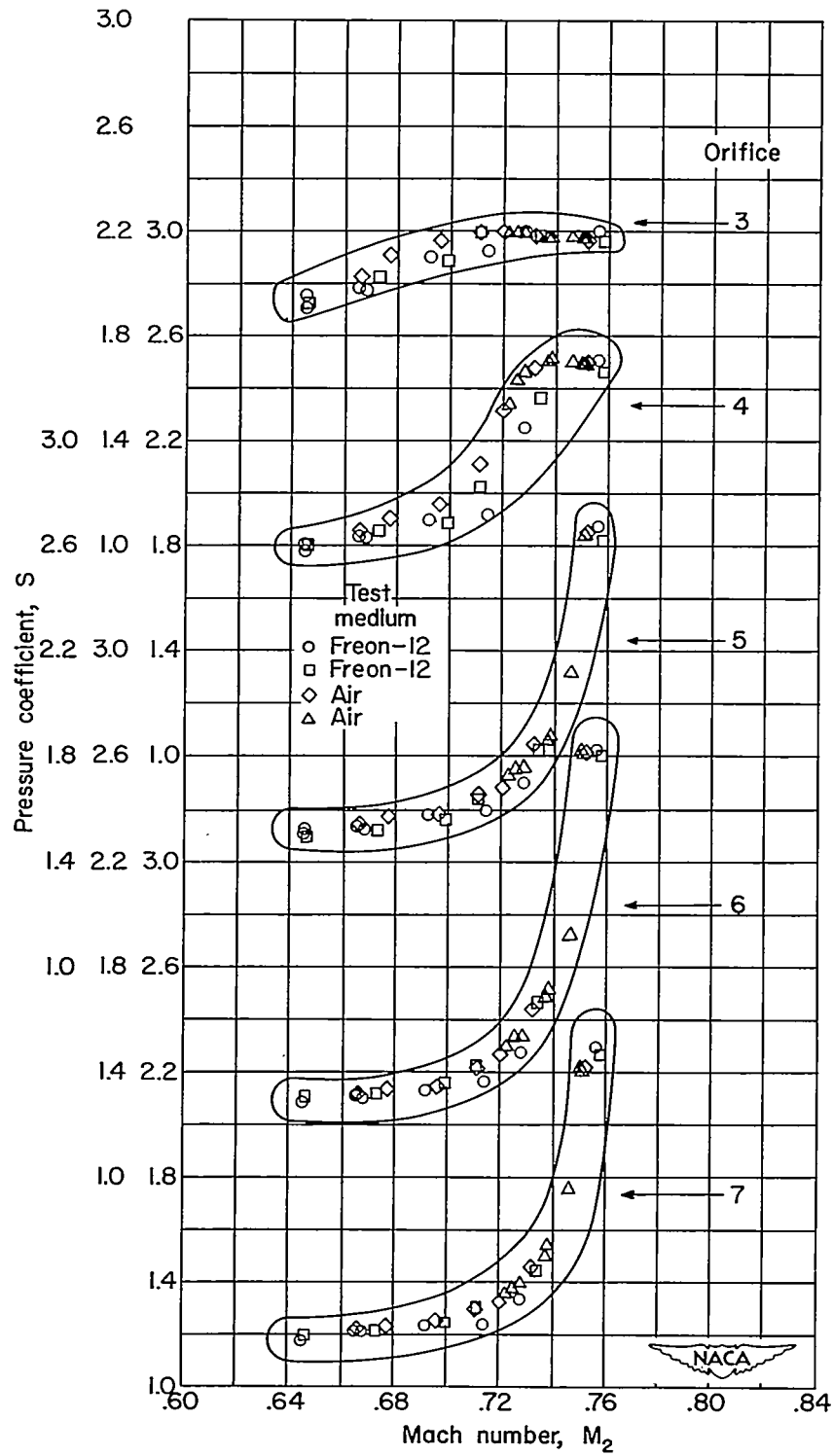


Figure 7.- Variation of pressure coefficient with  $M_2$  at each orifice location along the short bump. Freon data converted to equivalent air values.

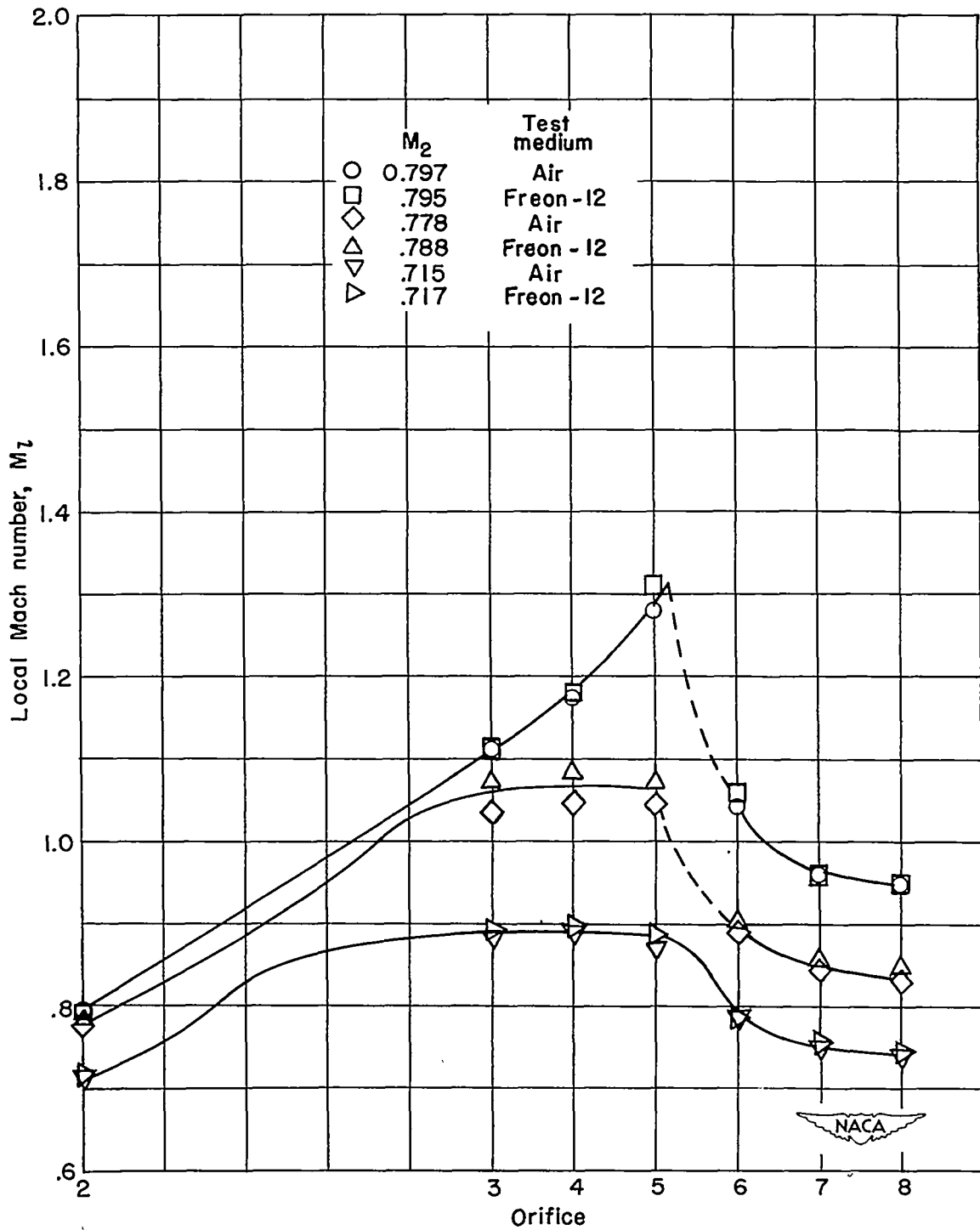


Figure 8.- Comparison of local Mach number distribution over long bump in Freon-12 and air. Freon-12 data converted to equivalent air values.

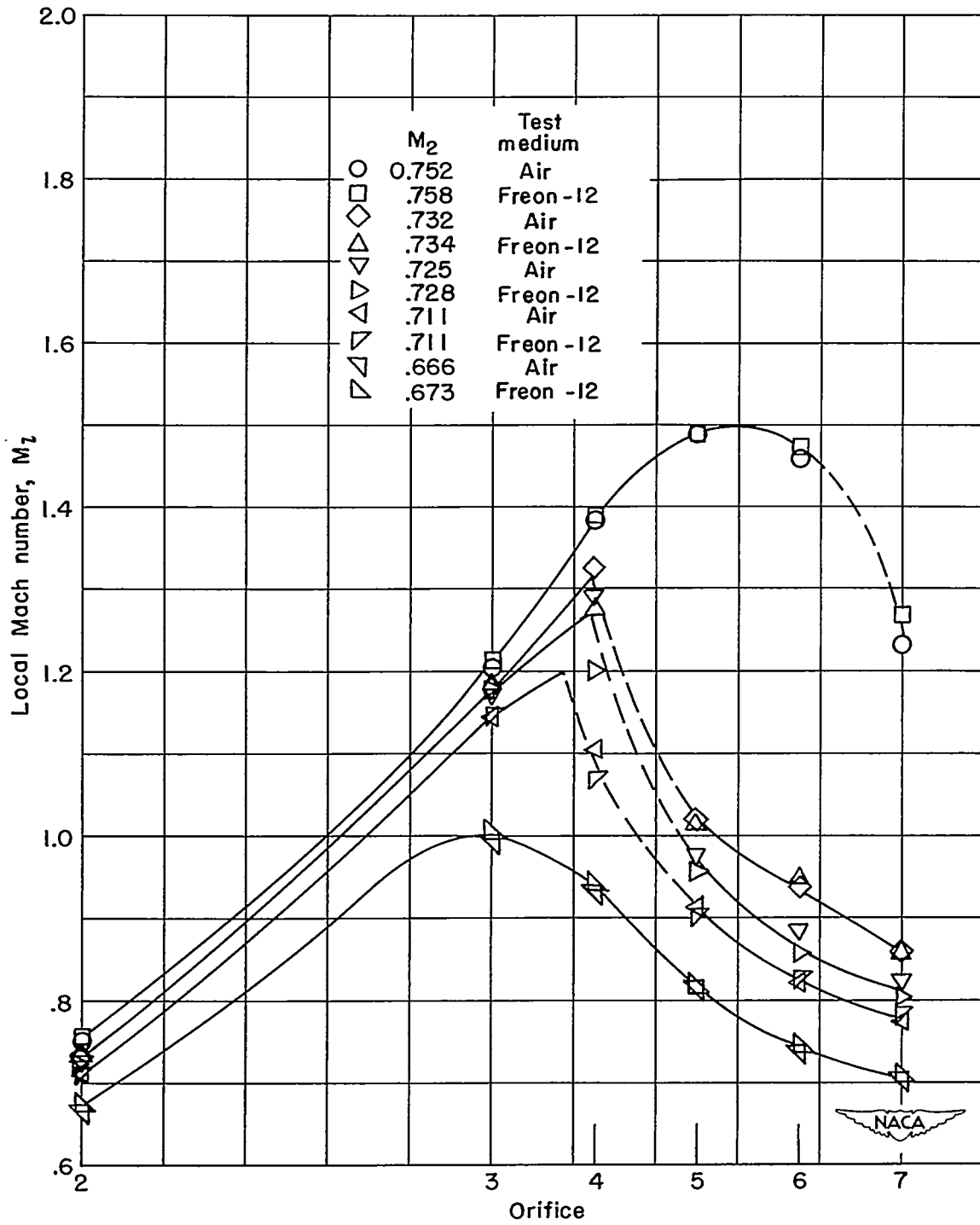


Figure 9.- Comparison of local Mach number distribution over short bump in Freon-12 and air. Freon-12 data converted to equivalent air values.

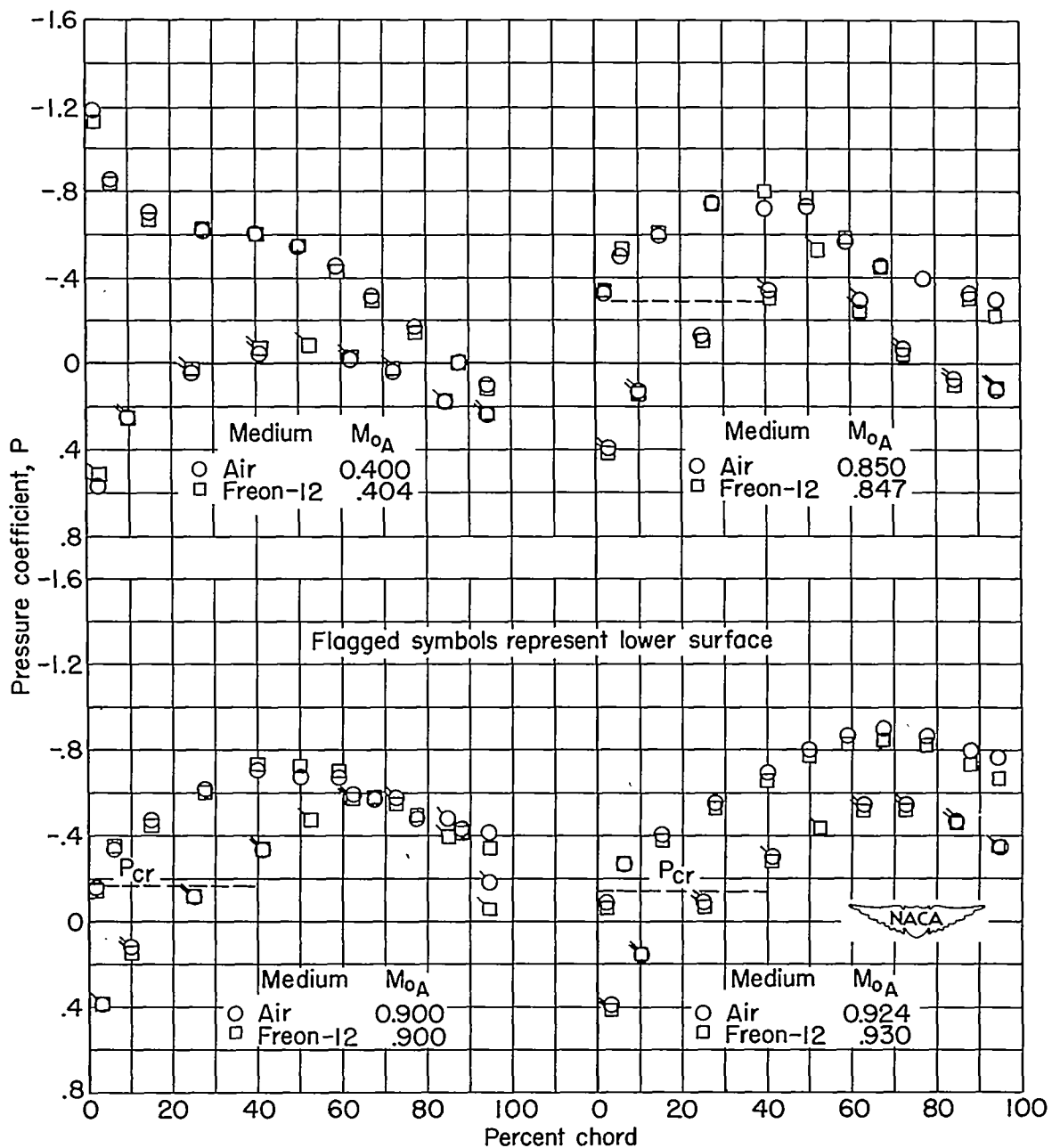


Figure 10.- Chordwise distributions of pressure at 30-percent semispan station of the NACA 65-210 wing.  $\Lambda = 0^\circ$ ;  $A = 9$ ;  $\lambda = 0.4$ ;  $\alpha = 4^\circ$ ; Freon-12 data converted to equivalent air values.

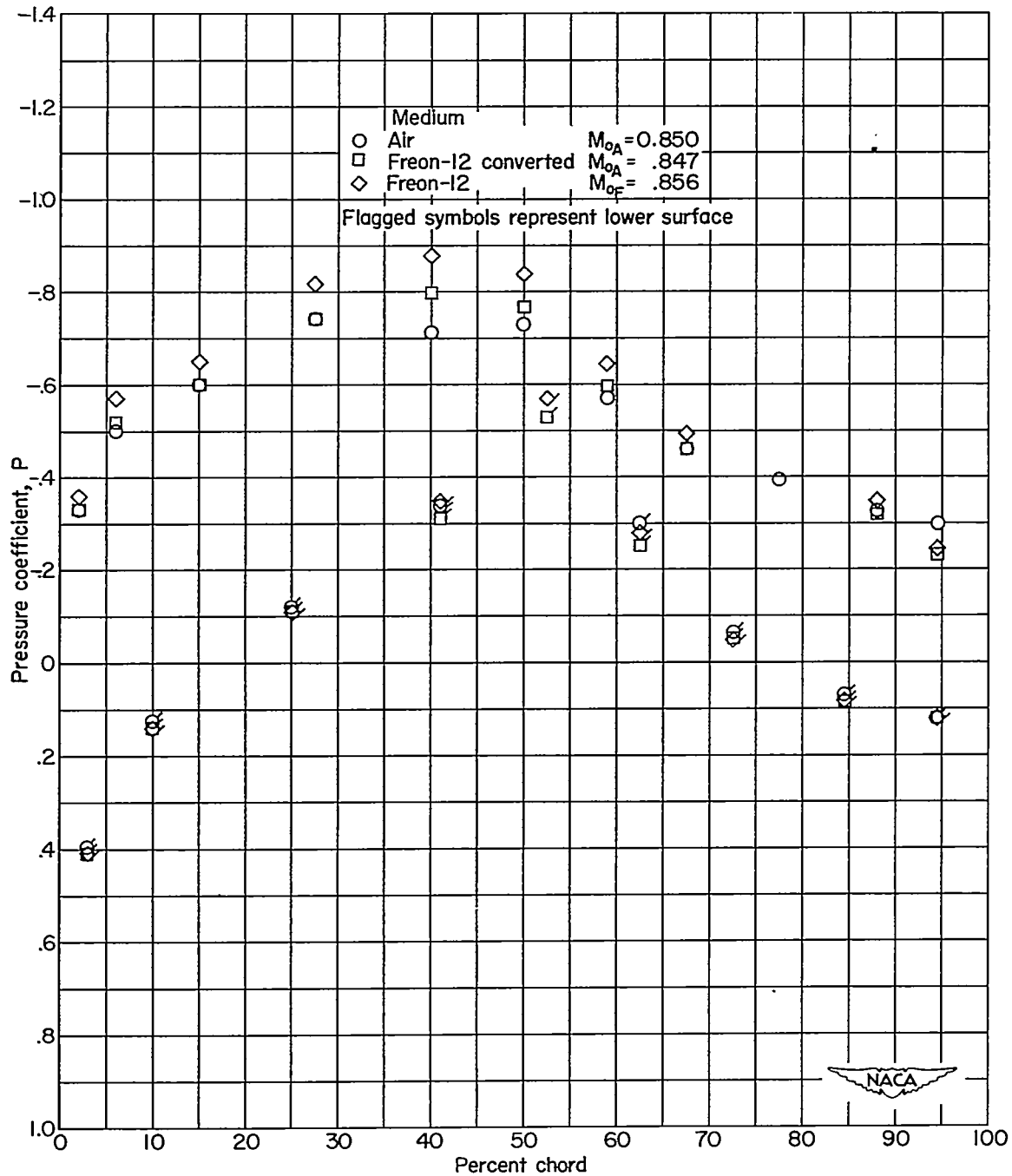
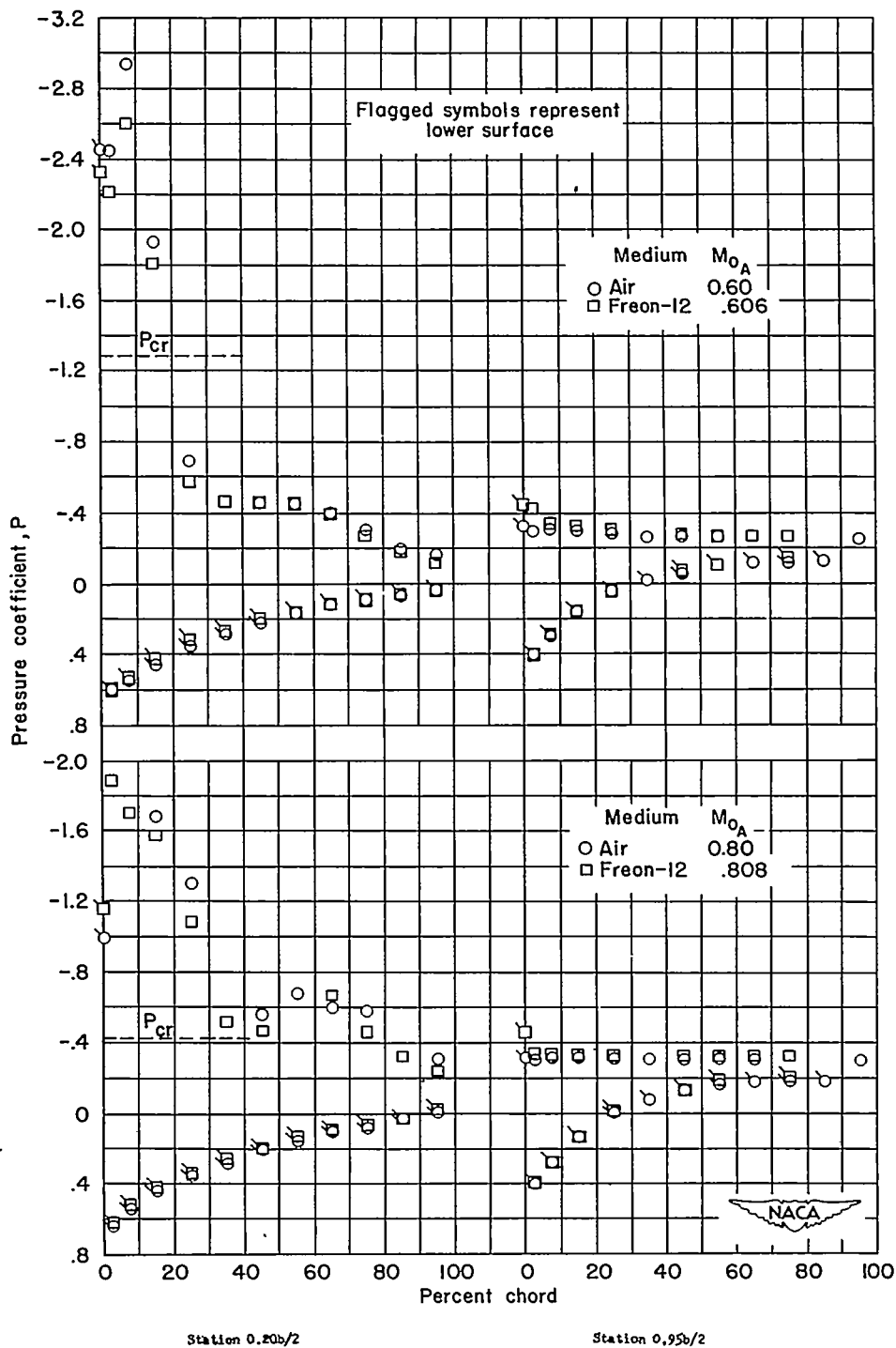
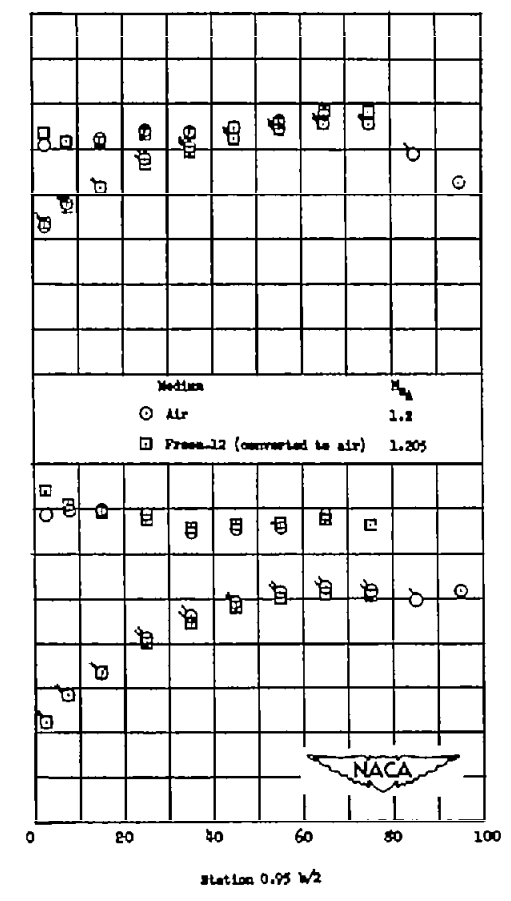
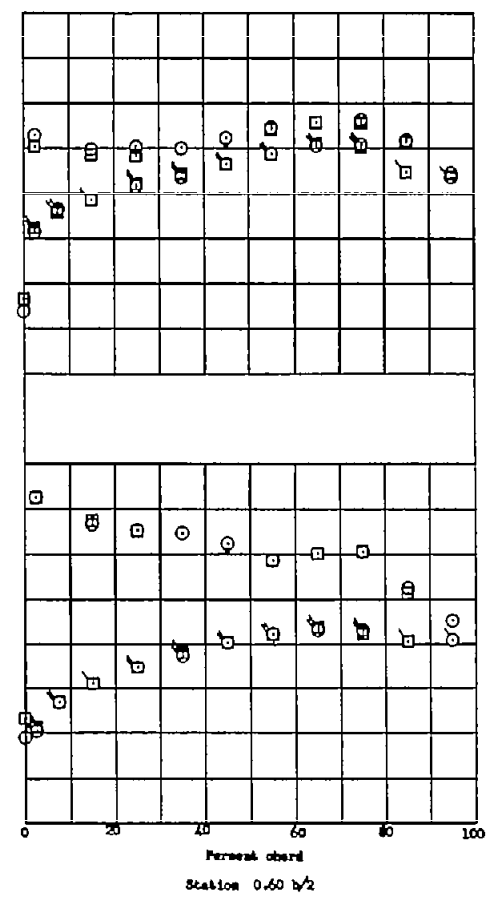
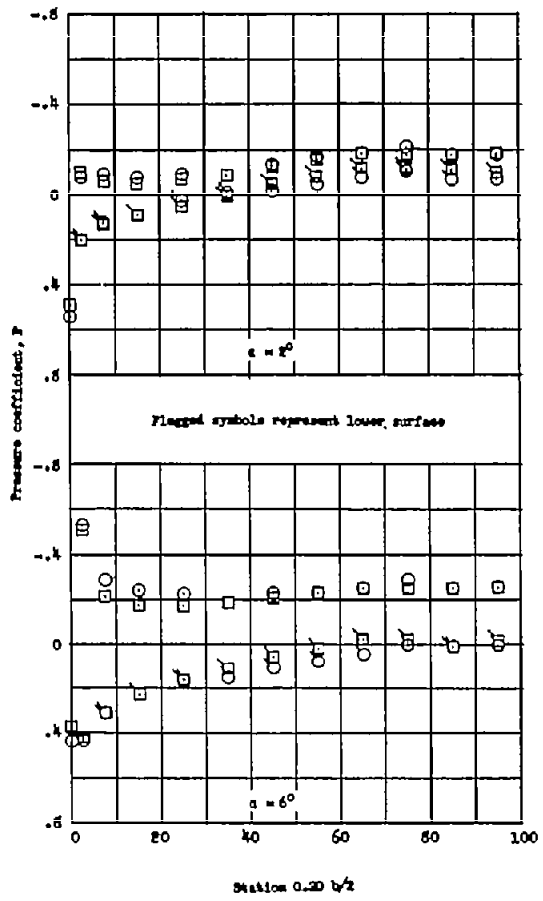


Figure 11.- Comparison of original and converted Freon pressure distributions with a corresponding pressure distribution measured in air. Configuration of figure 10.  $\Lambda = 0^\circ$ ;  $A = 9$ ;  $\lambda = 0.4$ ;  $\alpha = 4^\circ$ .

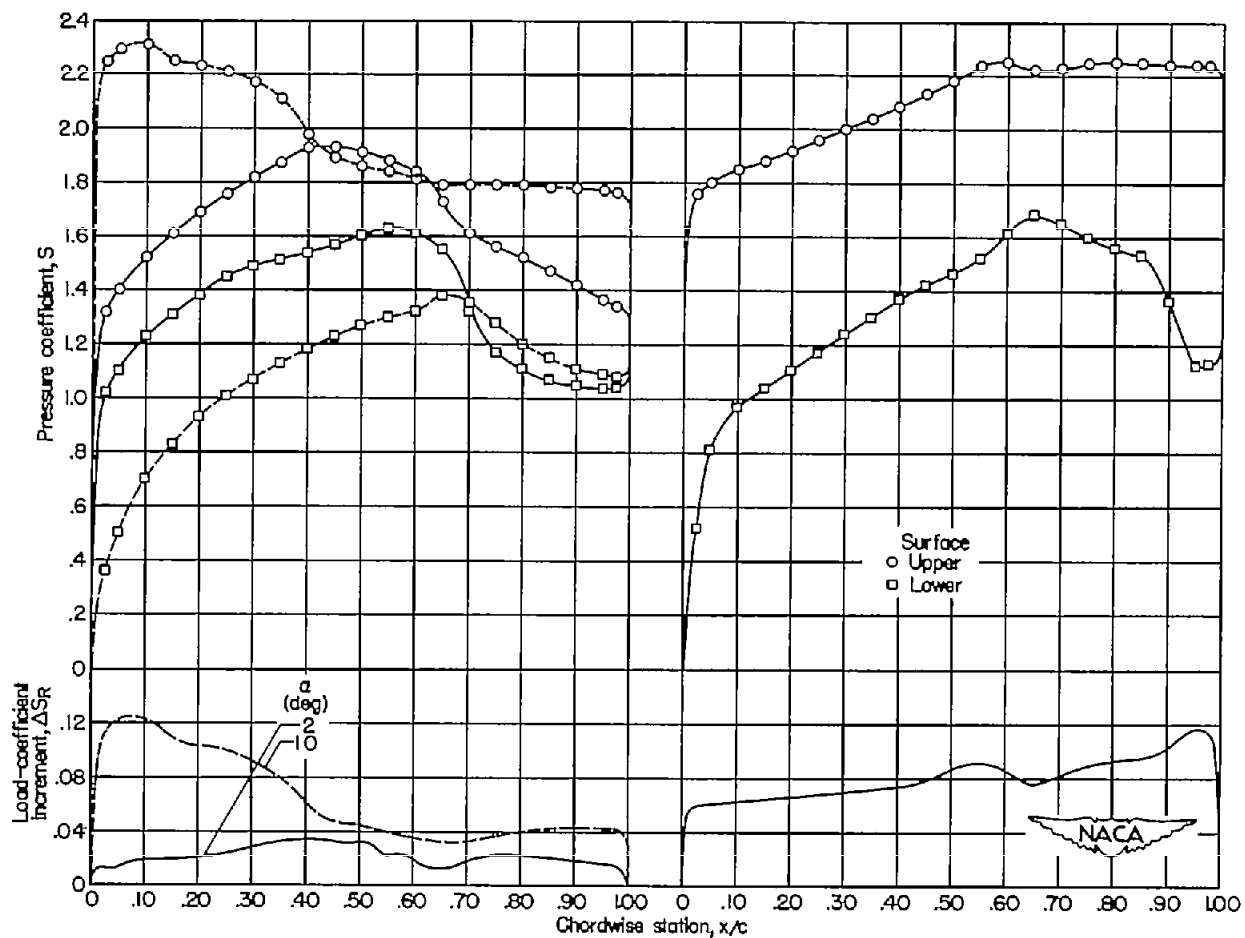


(a) Subsonic Mach numbers;  $\alpha = 14^\circ$ .

Figure 12.- Chordwise distributions of pressure at two semispan stations of the NACA 65A006 wing.  $\Lambda = 45^\circ$ ;  $A = 4$ ;  $\lambda = 0.6$ ; Freon-12 data converted to equivalent air values.



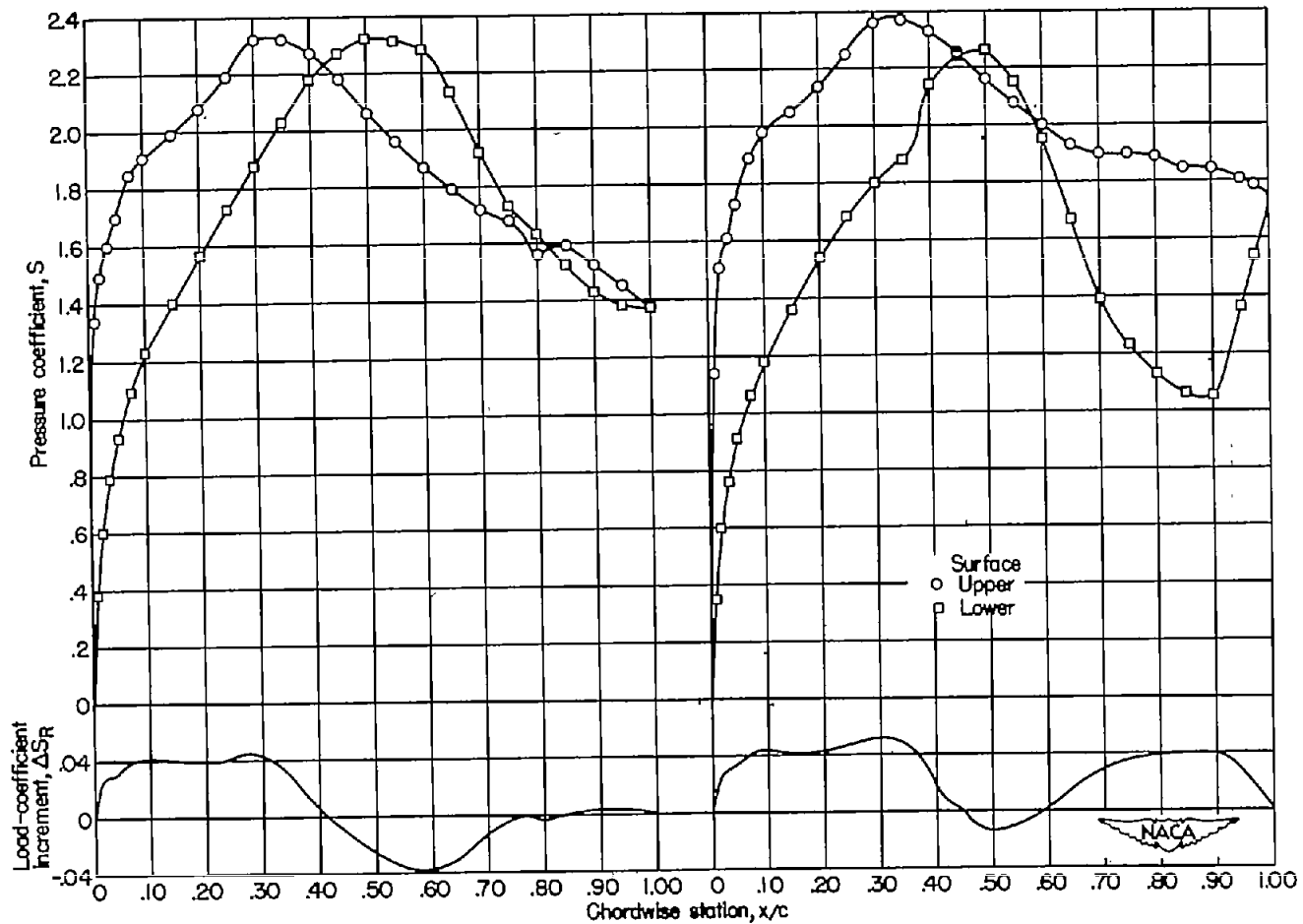
(b) Supersonic Mach number.  
 Figure 12.- Concluded.



(a)  $M_{0A} = 0.85$ ;  $\alpha = 2^\circ$  and  $-10^\circ$ .

(b)  $M_{0A} = 0.924$ ;  $\alpha = 7^\circ$ .

Figure 13.- Chordwise variation of upper- and lower-surface pressure coefficients in air and the calculated load-coefficient increments required to convert from air to Freon-12 for the NACA 65-210 airfoil.



(a)  $M_{0A} = 0.729$ ;  $\alpha = 4^\circ$ ;  $\delta = 0^\circ$ .

(b)  $M_{0A} = 0.729$ ;  $\alpha = 4^\circ$ ;  $\delta = 12^\circ$ .

Figure 14.- Chordwise variation of upper- and lower-surface pressure coefficients in air and the calculated load-coefficient increments required to convert from air to Freon 12 for the NACA 65,3-019 airfoil.

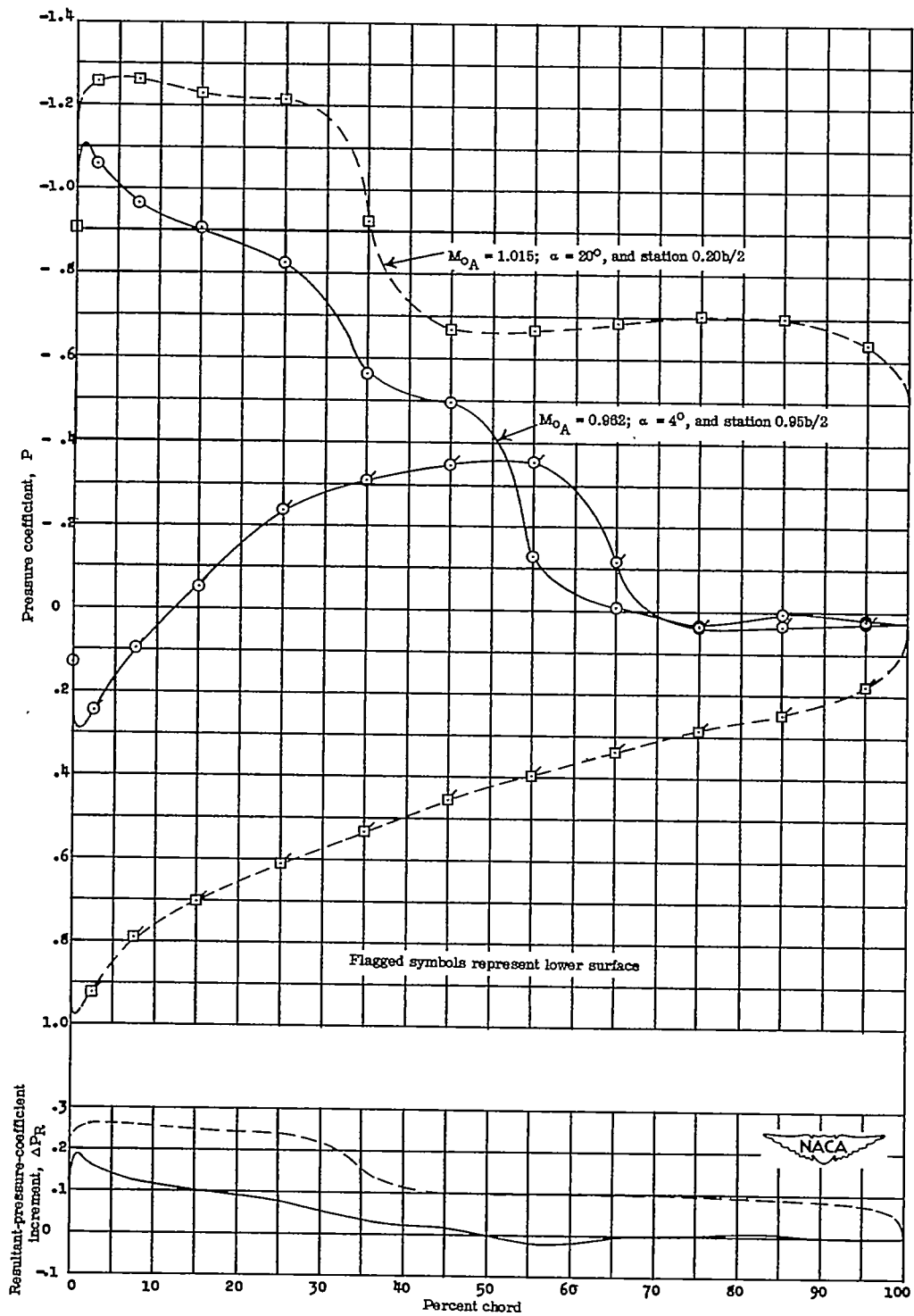


Figure 15.- Chordwise variation of upper- and lower-surface pressure coefficients in air and the calculated resultant-pressure-coefficient increments required to convert from air to Freon-12 for the NACA 65A006 airfoil.

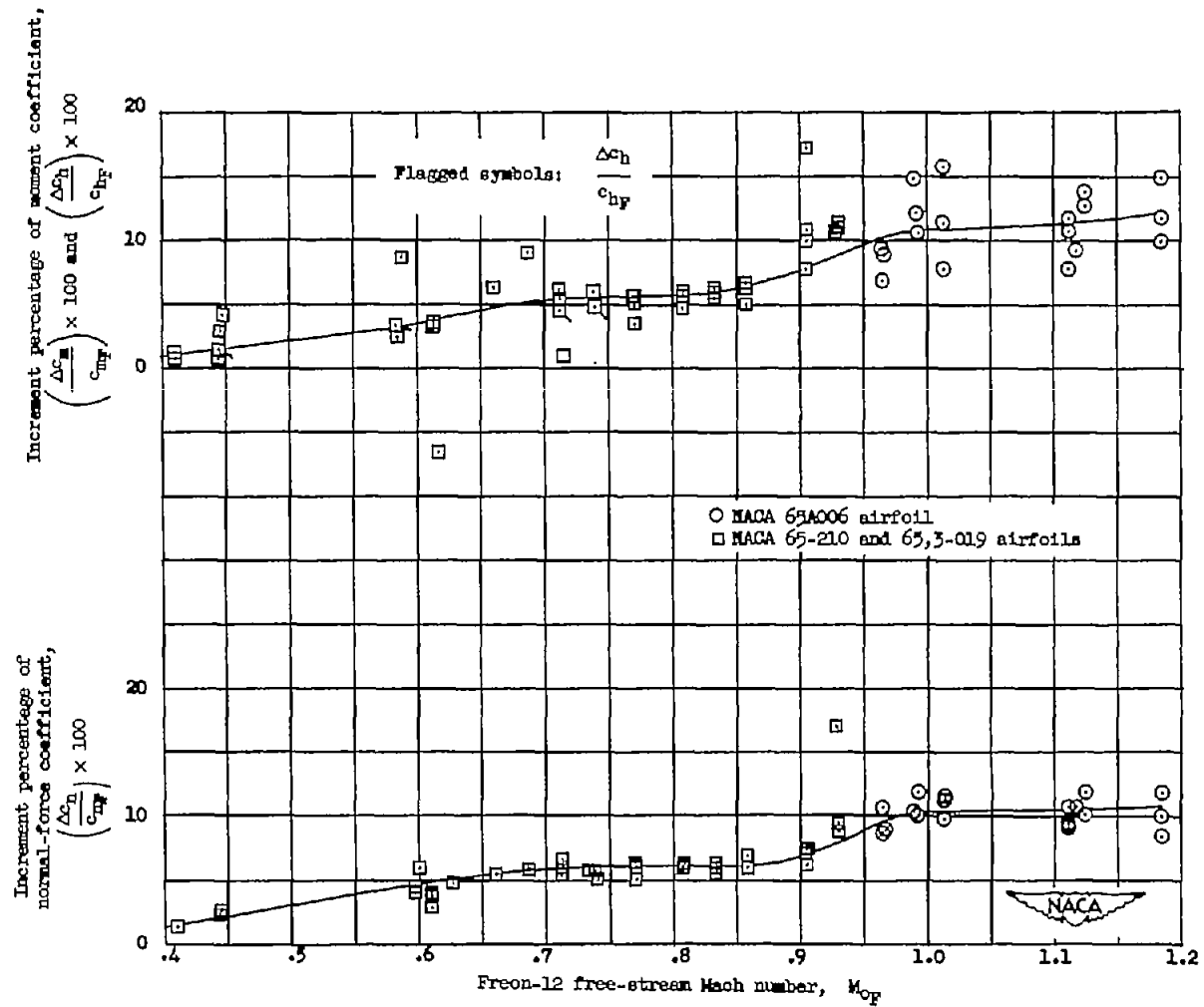


Figure 16.- Variation with Freon-12 free-stream Mach number of calculated increments required to convert lift and moment coefficients from Freon-12 to air.

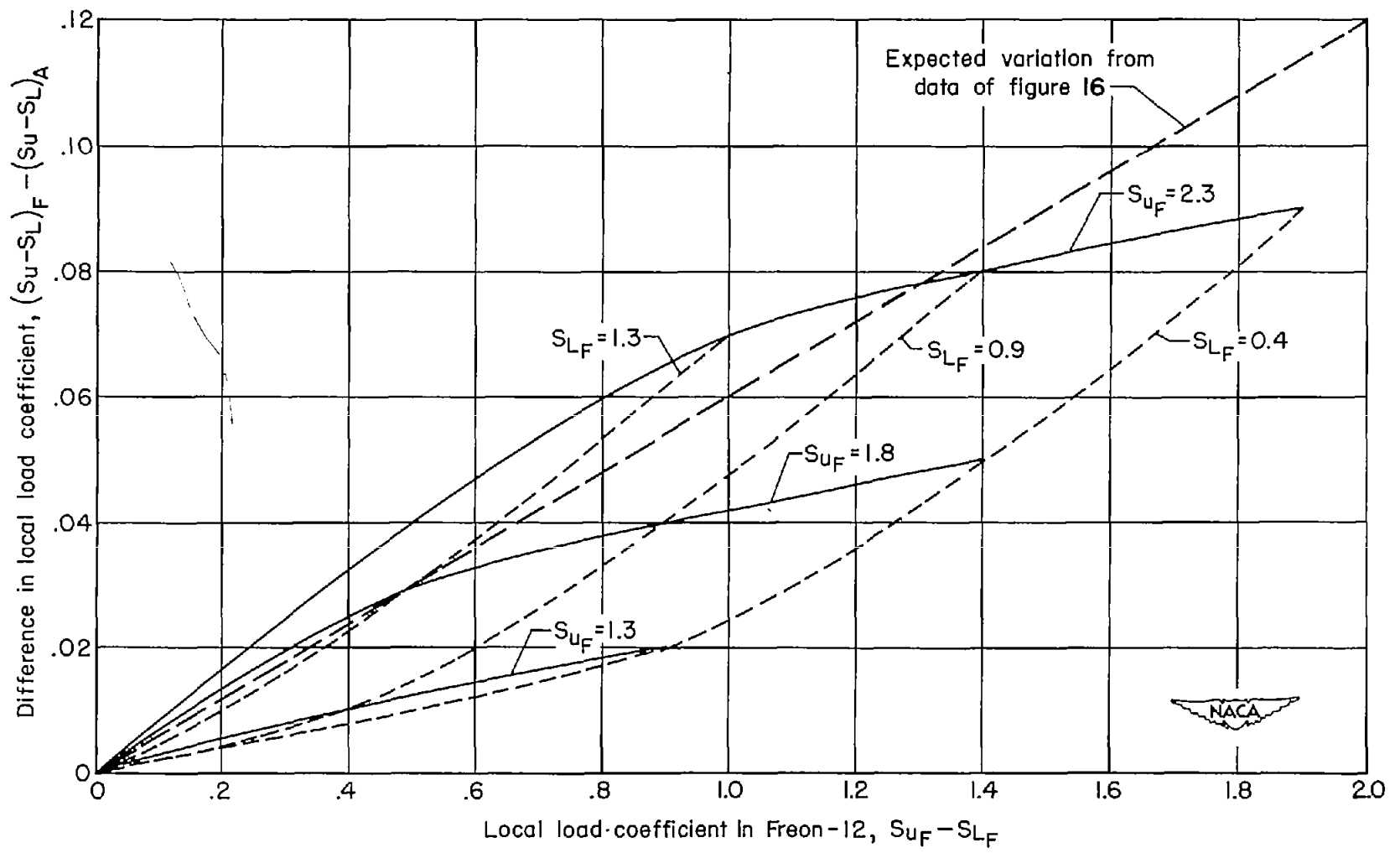


Figure 17.- Variation of difference in local load coefficient, as calculated by use of the streamline-similarity concept, with local load coefficient in Freon-12 for a free-stream Mach number of 0.80 in Freon.

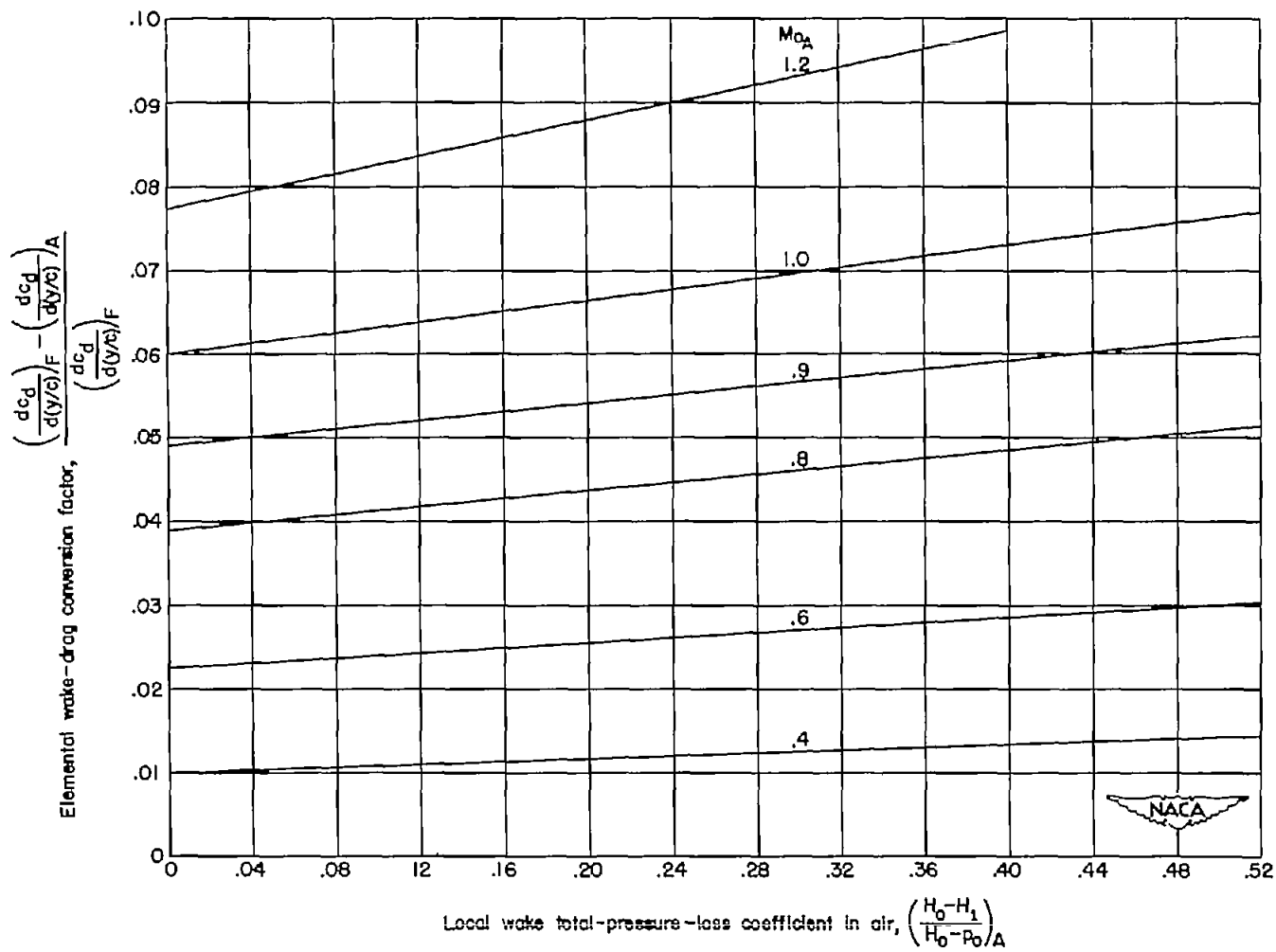


Figure 18.- Calculated variation of elemental wake-drag conversion factor with local wake total-pressure-loss coefficient in air for various free-stream Mach numbers in air.

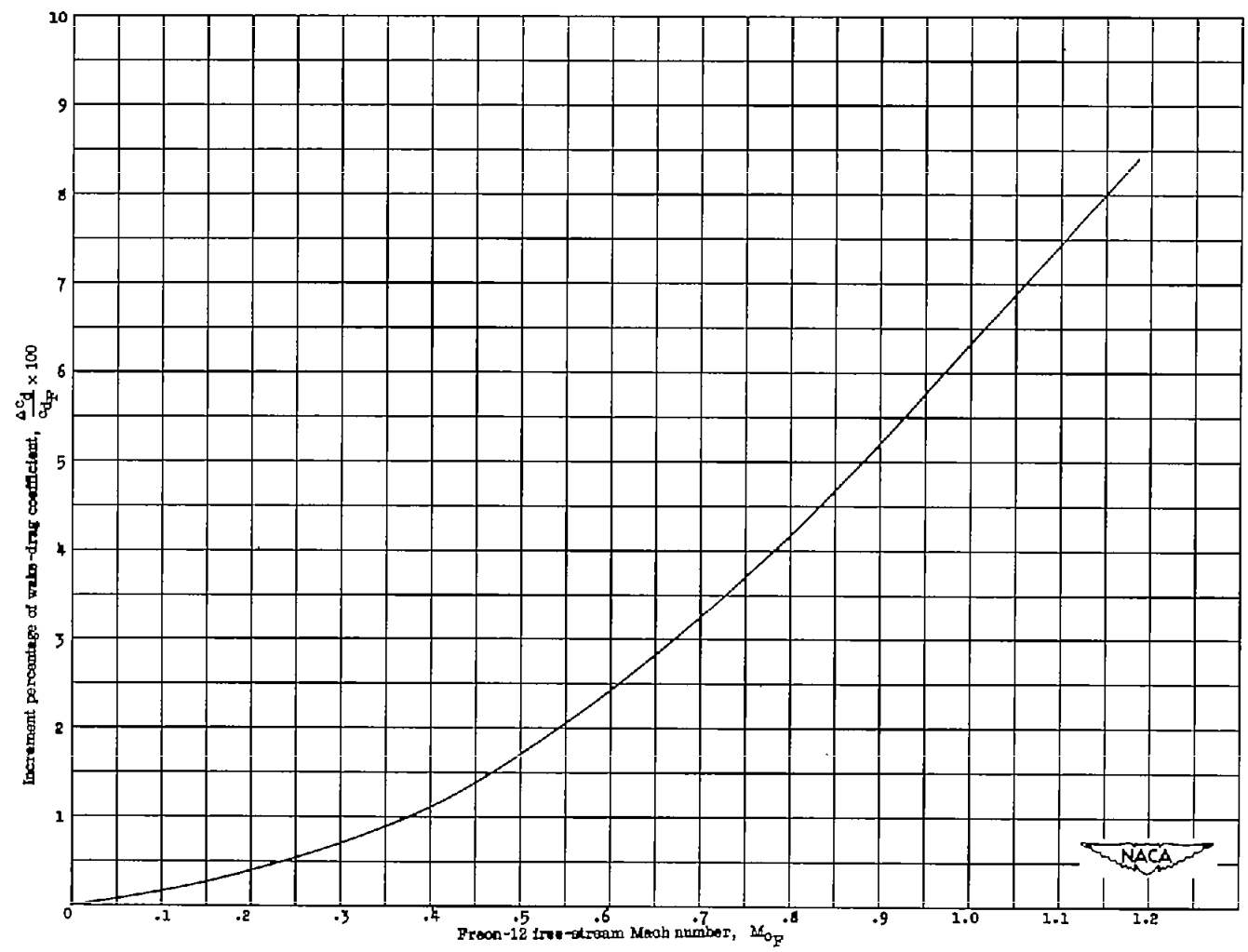


Figure 19.- Variation with Freon-12 free-stream Mach number of calculated increments required to convert wake drag coefficient from Freon-12 to air.

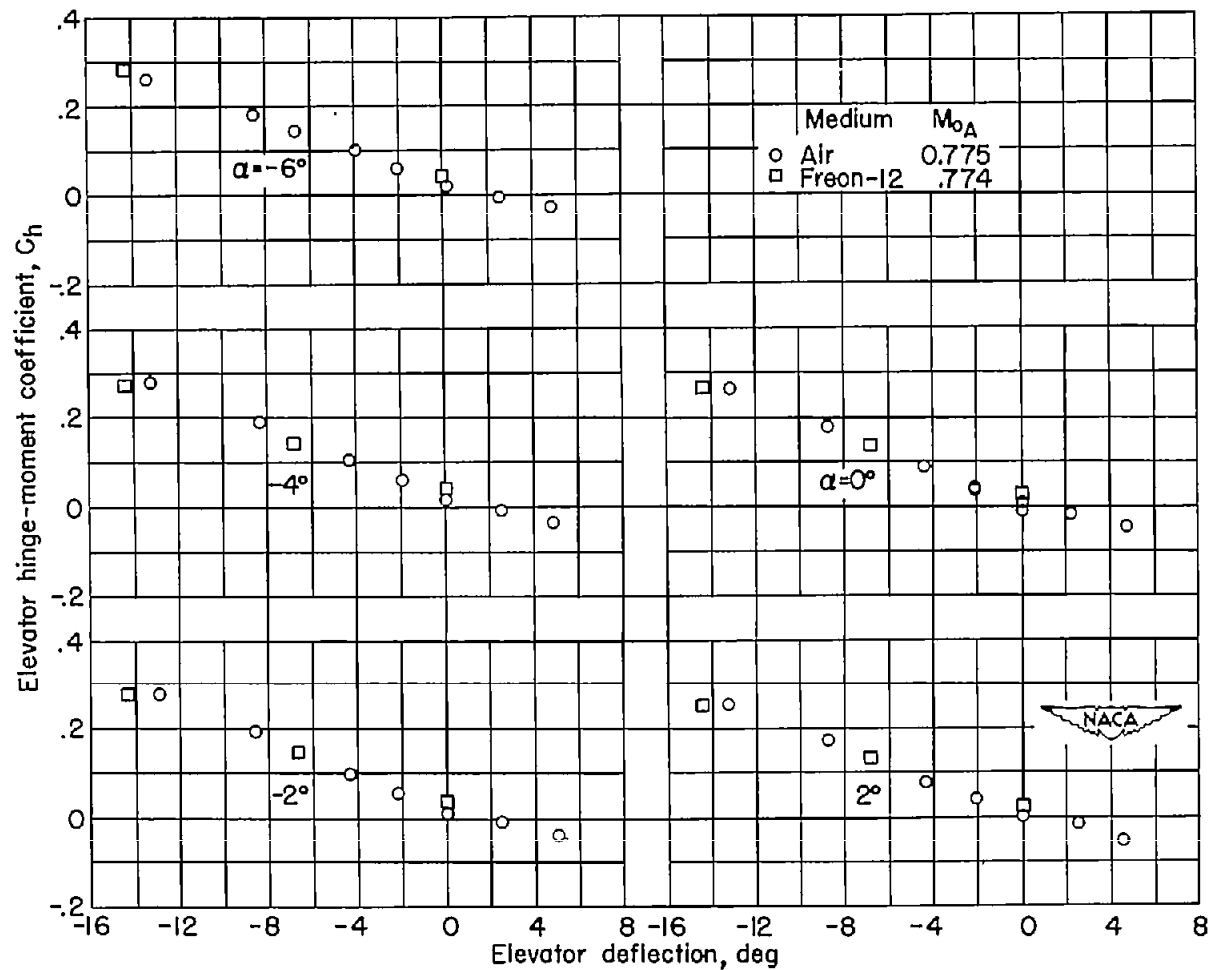
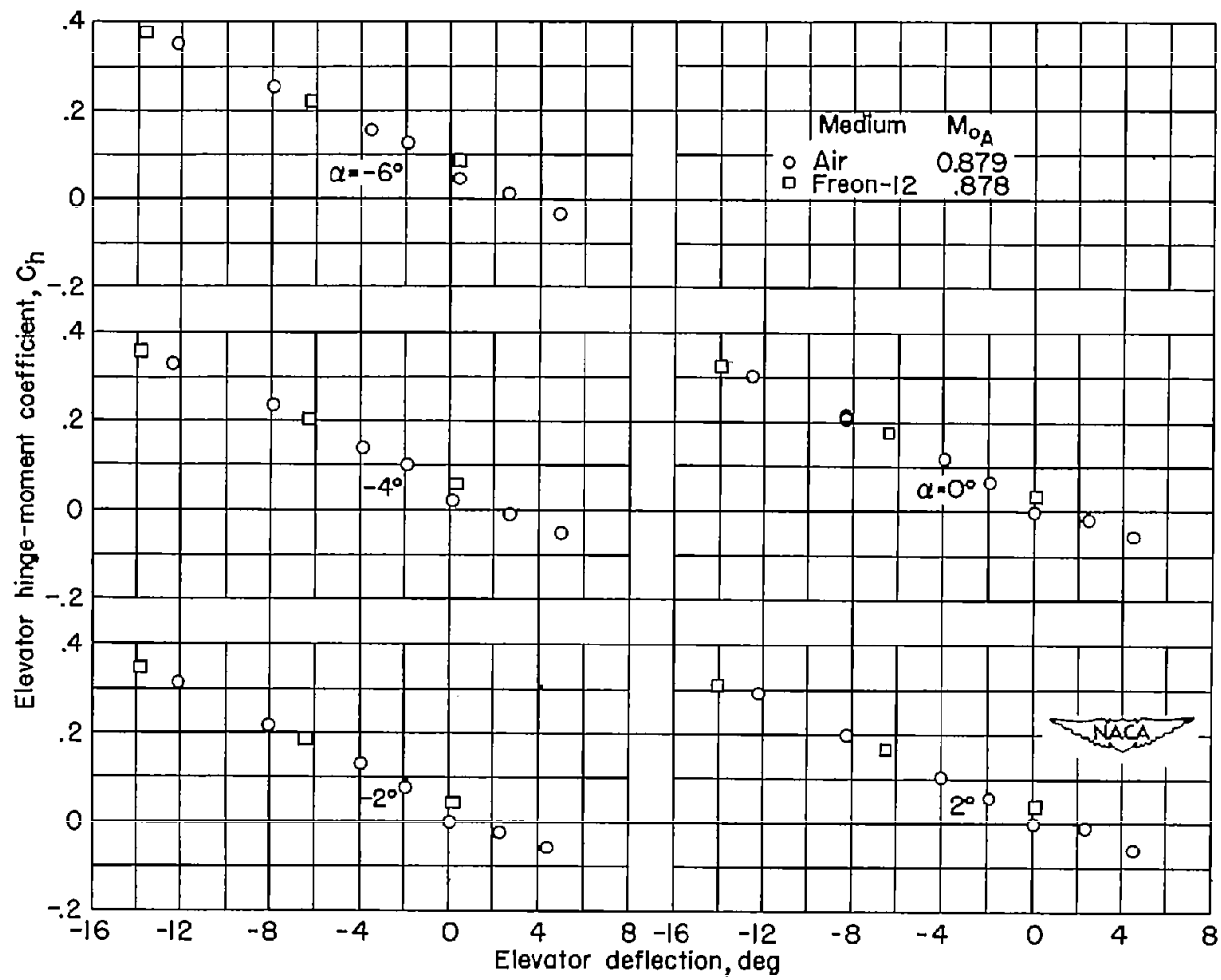
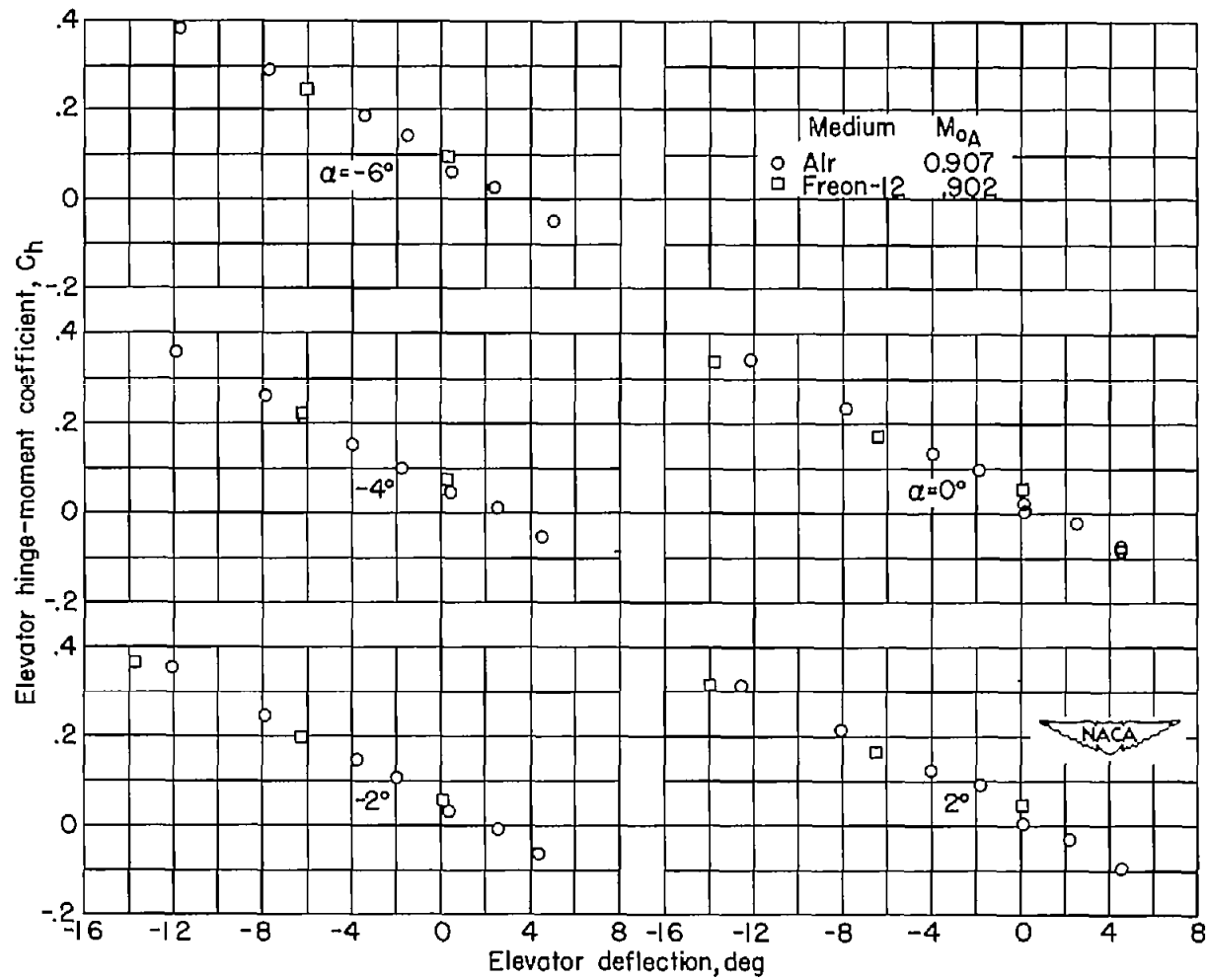
(a)  $M_{0A} = 0.775$ .

Figure 20.- Variation of elevator hinge-moment coefficient with elevator deflection for the NACA 65-108 tail surface.  $\Lambda = 0^\circ$ ;  $A = 4.01$ ;  $\lambda = 0.5$ ; Freon-12 data converted to equivalent air values.



(b)  $M_{oA} = 0.879$ .

Figure 20.- Continued.



(c)  $M_{0A} = 0.907$ .

Figure 20.- Concluded.

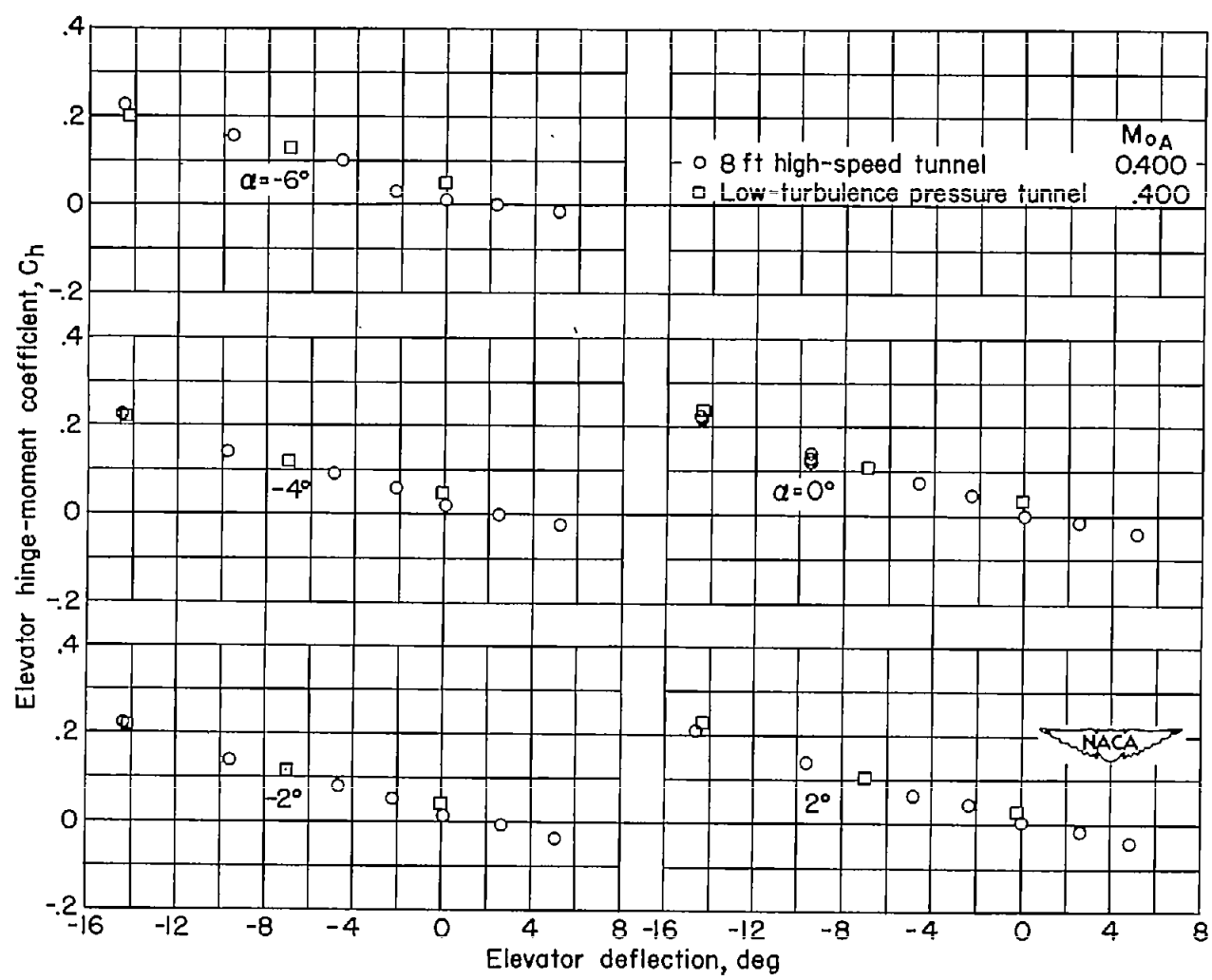


Figure 21.- Variation of elevator hinge-moment coefficient with elevator deflection as obtained only in air. Configuration of figure 20.  $\Lambda = 0^\circ$ ;  $A = 4.01$ ;  $\lambda = 0.5$ .

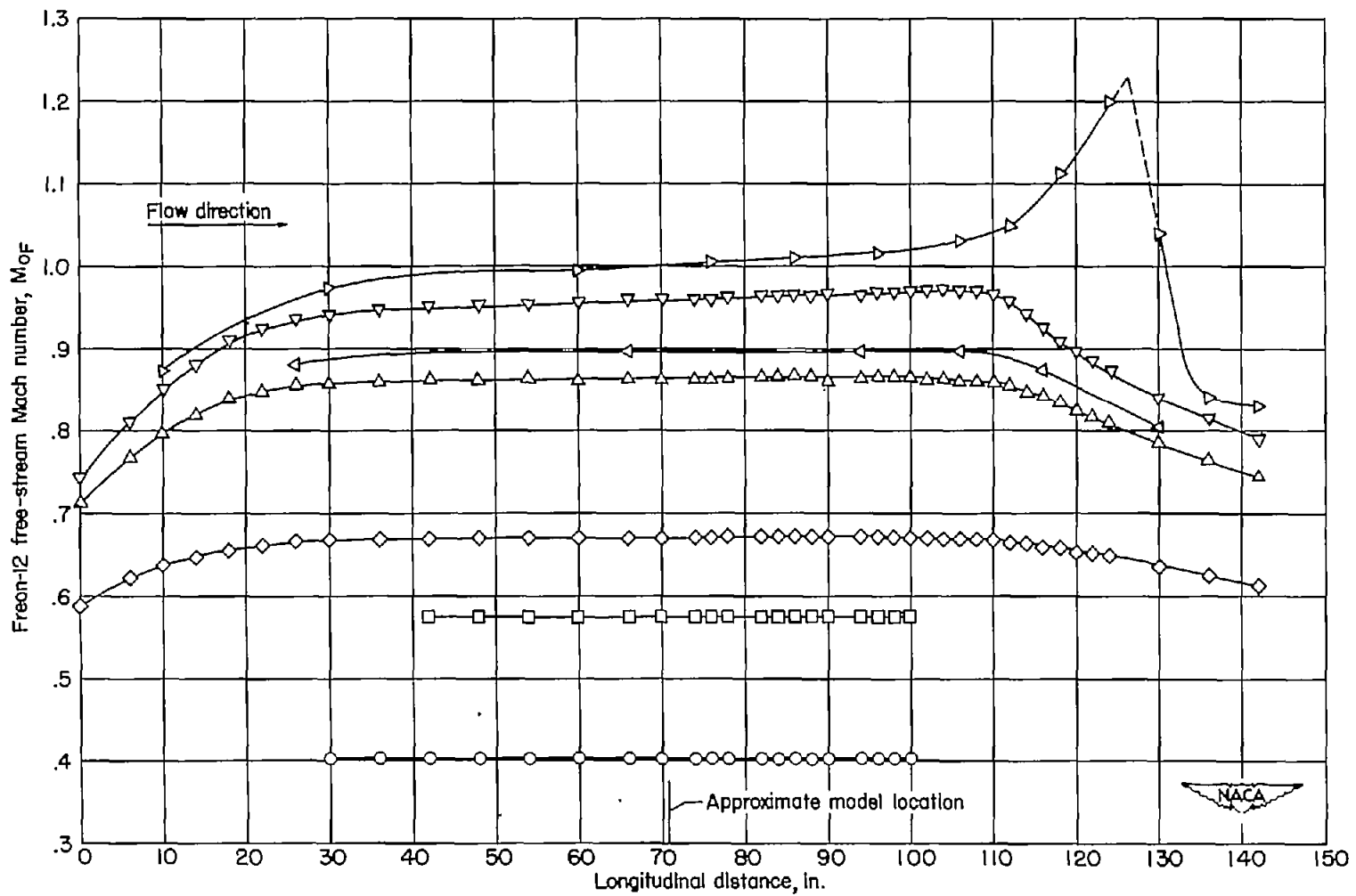


Figure 22.- Longitudinal distribution of Mach number along the center line of the Langley low-turbulence pressure tunnel with Freon-12 as a test medium.

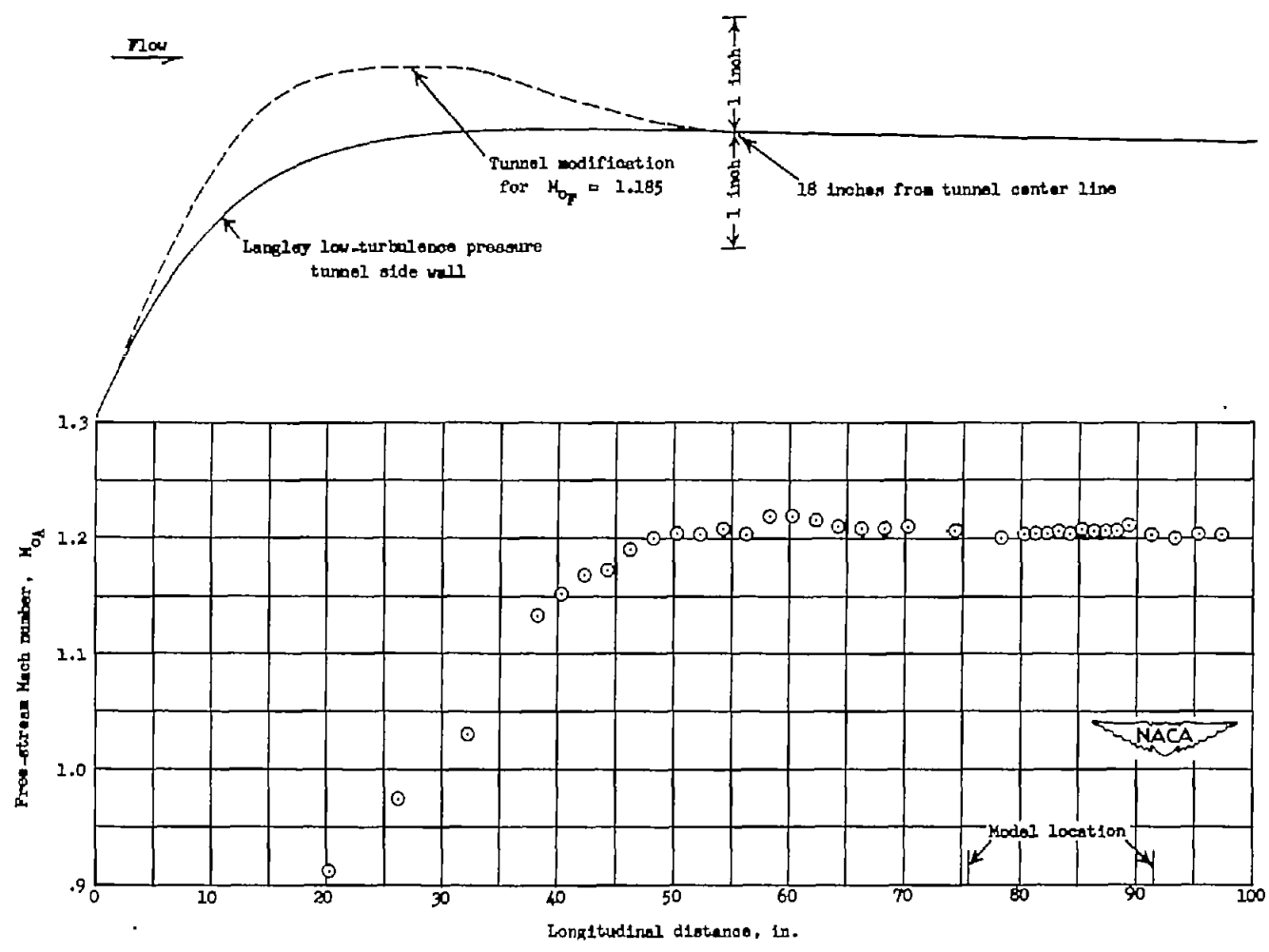


Figure 23.- Longitudinal distribution of Mach number midway between the center line and the side wall of the Langley low-turbulence pressure tunnel with the plaster liner installed and Freon-12 as the test medium. Freon-12 data converted to air values.

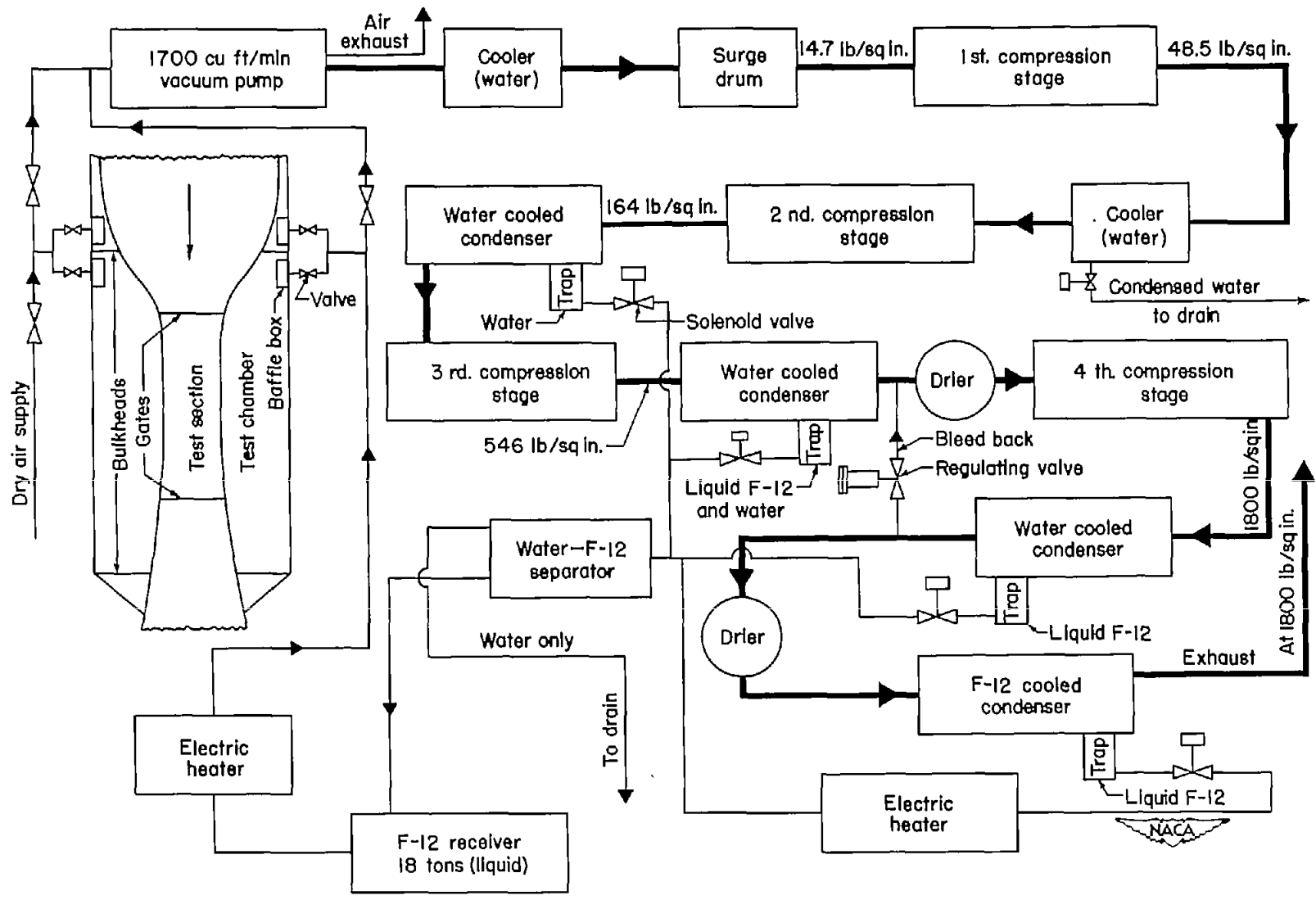


Figure 24.- Schematic diagram of Freon-12 recovery system.

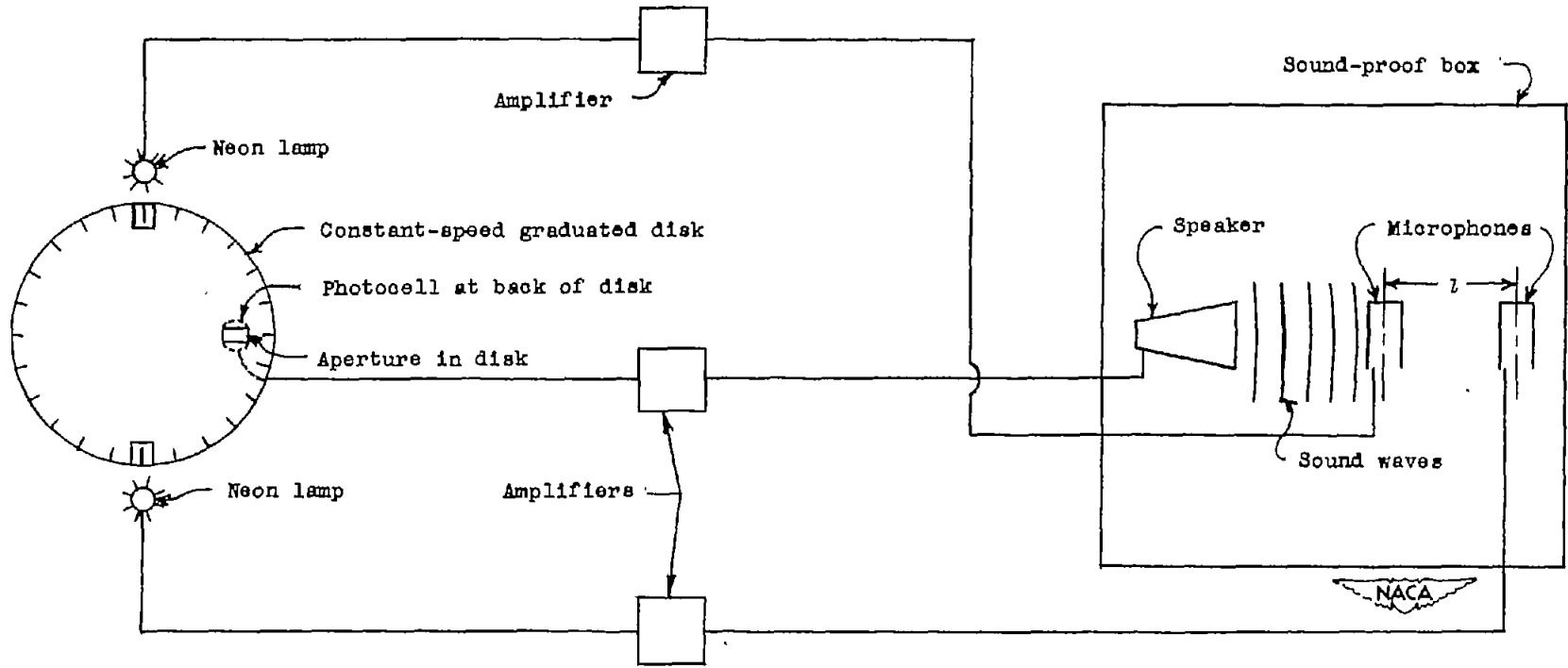


Figure 25.- Schematic diagram of Freon-12 purity meter.